Degradation of lithium-ion batteries: a meta-analysis

Matteo Ligorati, Jerome Geyer-Klingeberg, Timon E. Günther, Andreas W. Rathgeber

Angaben zur Veröffentlichung / Publication details:

Ligorati, Matteo, Jerome Geyer-Klingeberg, Timon E. Günther, and Andreas W. Rathgeber. 2026. “Degradation of lithium-ion batteries: a meta-analysis.” *Chemical Engineering Journal*. https://doi.org/10.1016/j.cej.2026.174528.

Journal Pre-proof

Degradation of lithium-ion batteries: A meta-analysis

Matteo Ligorati, Jerome Geyer-Klingeberg, Timon E. Günther, Andreas W. Rathgeber

PII: S1385-8947(26)01987-X

DOI: https://doi.org/10.1016/j.cej.2026.174528

Reference: CEJ 174528

To appear in:

Received date: 17 November 2025

Revised date: 16 February 2026

Accepted date: 22 February 2026

Please cite this article as: M. Ligorati, J. Geyer-Klingeberg, T.E. Günther, et al., Degradation of lithium-ion batteries: A meta-analysis, (2024), https://doi.org/10.1016/j.cej.2026.174528

Degradation of lithium-ion batteries: a meta-analysis

Matteo Ligorati[a], Jerome Geyer-Klingeberg[a], Timon E. Günther[b], and Andreas W. Rathgeber[a]

[a] Professorship for Applied Data Analysis, Institute of Materials Resource Management, University of Augsburg, Am Technologiezentrum 8, 86159 Augsburg, Germany

[b] Department of Resource and Chemical Engineering, Institute of Materials Resource Management, University of Augsburg, Am Technologiezentrum 8, 86159 Augsburg, Germany

˜Corresponding author: matteo.ligorati@uni-a.de (M. Ligorati), Tel.: +49 821 598 – 69205

Abstract

The transition toward sustainable energy systems requires reliable and durable energy storage technologies, with lithium-ion batteries (LIBs) being central to electrification and the integration of renewables. However, the decline in capacity per cycle, referred to as the degradation rate (DegRate), decreases the lifetime and performance of LIBs, thereby limiting their ecological and economic benefits. To address this, we conducted the first meta-analysis of LIB degradation, drawing on 146 studies and 917 effect sizes. The analysis accounts for the heterogeneity in reported DegRates using explanatory variables grouped into battery differences, experiment-, measurement-, and publication-specific categories. Across studies, we found a median DegRate of 0.04 %/cycle, with cut-off charge voltage and temperature emerging as the dominant influencing factors. Using meta-regression, we quantify the effects of these explanatory variables. Furthermore, we establish a forward-looking quantitative benchmark: under extreme cold (<0 °C) and very high charge cut-off voltages, model-implied mean DegRates for graphite-based systems reach 0.68–1.41 %/cycle (14–29 cycles). For promising Si-based chemistries, the benchmark is more prospective with model-implied mean DegRates of 0.98 – 1.71 %/cycle (11–20 cycles), with higher uncertainty in these sparsely covered regimes, as reflected in the confidence intervals. This study highlights critical gaps in the experimental matrix and, rather than relying on a single estimate, establishes quantitative benchmarks for LIB degradation that serve as a reference for future research, particularly for combinations of operating conditions that have not yet been experimentally explored.

Keywords: Lithium-ion battery, Degradation rate, Determinants, Cycle life estimation, Meta-analysis

Abbreviations	
BMA	Bayesian model averaging
CI	Confidence interval
CV	Constant voltage
DegRate	Degradation rate
DoD	Depth of discharge
EoL	End-of-life
Eq.	Equation
LIB	Lithium-ion battery
MCMB	Mesocarbon microbeads
MRA	Meta-regression analysis
PICOS	Population, Intervention, Comparison, Outcomes, Study design
PIP	Posterior inclusion probabilities
PMP	Posterior model probabilities
Post	Posterior
PRISMA	Preferred Reporting Items for Systematic Reviews and Meta-Analyses
SD	Standard deviation
SEI	Solid electrolyte interphase
Si-based	Silicon-based
SoC	State of charge
Std. Dev.	Standard deviation
UW	Unweighted
VIF	Variance inflation factors
WLS	Weighted least squares

1 Introduction

Lithium-ion batteries (LIBs) have become the cornerstone of modern energy storage systems. With high energy density, and long cycle life, they are applicable in various applications. However, the performance and ultimate lifespan of LIBs are subject to limitations determined by cathode/anode chemistry**,** multiple cell formats, such as pouch, cylindrical, or coin cells, and operational parameters like charge/discharge behavior [1–5]. Understanding and quantifying the degradation mechanisms is therefore essential to improve LIB-systems and extend their lifespan. Thermal instability and side reactions at the electrode-electrolyte interface contribute to capacity loss and safety risks as recent studies show [6–8]**.** Especially the development of advanced electrode materials is focus of scientific work, with intercalation-type materials like $LiCoO_2$ (LCO)**,** $LiFePO_4$ (LFP), and $LiNi_{0.8}Mn_{0.1}Co_{0.1}O_2$ (NMC811**)** dominating current LIBs due to their structural stability and reversibility with extended lifespan and flexible charge-discharge ability. Recent reviews have also highlighted the emergence of nanostructured and doped materials, as well as high-nickel containing cathodes and silicon-based (Si-based) anodes, which aim to overcome the limitations of traditional materials and meet the growing demand for high-performance and sustainable batteries [9–11]**.** While a large body of literature describes these physicochemical processes (among others, [6–8]), Dechent et al. [9] present an approach to visualize lithium-ion cells in an energy-power plane, encoding lifetime via energy-throughput- and full-equivalent-cycle-based indicators and cycling temperature across different electrode materials. However, despite such large-scale syntheses that summarize lifetime trends, the marginal effect of specific drivers remains unquantified. In particular, it is currently unclear how much degradation is driven by internal (material/cell format) versus external (operational) factors when both are statistically controlled simultaneously, given the accumulated heterogeneity across experimental studies. This heterogeneity arises from differences in experimental design, measurement approaches, and battery-specific characteristics, which together lead to substantial variation in degradation rate (DegRate). The present meta-analysis aims to identify the factors most responsible for this variability.

To the best of our knowledge, we present the first meta-analysis in the field of battery degradation. Meta-analysis is an established method for secondary research with applications in medicine [10–13], economics [14–18], and engineering [19–29], among others. By comparing experimental data, operating conditions, and diagnostic techniques, this study quantifies battery degradation mechanisms and performance loss over time, as well as highlighting current gaps in research. Thereby, the cumulating effects that affect lifetime, cycle stability**,** and loss of capacity can be distinguished and traced back**.**

A LIB consists of a graphite anode, a lithium metal oxide cathode (e.g., $LiCoO_2$, $LiFePO_4$ or $Ni_{0.8}Mn_{0.1}Co_{0.1}O_2$), a porous separator, and an organic liquid electrolyte (e.g., $LiPF_6$). During discharge, as shown in Figure S1, lithium-ions migrate from the anode through the electrolyte to the cathode while electrons are conducted in an external circuit to the consumer delivering electrical energy (Eq. (1)). This process is reversed during charging (Eq. (2)).

Discharge:

$$Li_y\,M \leftrightarrow Li_x\,M^{n+} + ne^- \quad (1)$$

Charge:

$$Li_x\,M^{n+} + ne^- \leftrightarrow Li_y\,M \quad (2)$$

Whereas $Li_x\,M^{n+}$ is the oxidized/discharged state of the cathode material (M = Ni, Co, Mn, Al,...), n is the number of transferred electrons and $Li_y\,M$ is the reduced/charged state of the anode material [8]. The electrochemical performance of the battery varies strongly depending on the choice of active materials (anode, electrolyte, cathode), cell format **(**e.g., pouch, cylindrical, prismatic, or coin), charge-discharge behavior and cell environment (temperature)**.** Recent progress was made with solid-state electrolytes, silicon-based electrodes and high-nickel cathodes such as NMC to improve energy density and safety [30].

Strategies to enhance the performance of LIBs are dimension reduction, composite formation, doping, morphology control, thin film coating and encapsulation or electrolyte modification as Nitta et al. [30] report early [8,31]. A breakthrough was made with the development of commercial intercalation materials such as lithium cobalt oxide (LCO), lithium nickel cobalt manganese oxide (NMC), lithium nickel cobalt aluminum oxide (NCA), lithium iron phosphate (LFP) or lithium titanium oxide (LTO). In contrast, conversion materials like alloyed anodes (Si, Ge, Sn) or metal halides (F, Cl, Br, I) show good performance. Specific capacities of 80 to 230 mAh/g can be reached [32]. Du et al. [32] report that in an ideal lithium battery system, the only occurring physicochemical process is the shuttling of lithium-ions between anode and cathode. Unfortunately, several side reactions and other processes occur in state-of-art batteries. Those degradation processes result from the interaction between internal factors such as cell format, choice of cathode, anode and electrolyte, and external and operational factors such as temperature, C-rate, state of charge (SoC) and depth of discharge (DoD). Thereby induced irreversible reactions in the electrochemical cell, with change of material composition, lead to lowering cell voltage and capacity, therefore cycle number and lifetime of the battery.

In detail, loss of active material, graphite exfoliation, Al-foil corrosion and electrolyte decomposition can be caused by thermal instabilities, mechanical stress, deep discharging or overcharging, forcing side reactions at the SEI with loss of capacity, and impedance growth [30,32]. More information on the occurring degradation processes is available in the Supplementary Material (S.2).

To evaluate the relation between the internal and external effects on DegRate of the battery cells, quantitative data from experimental studies were collected and clustered in this study as shown in Figure 1.

Although lithium-ion battery degradation has been extensively studied in primary experiments and narrative reviews, the field lacks a systematic, quantitative synthesis that standardizes outcomes across

heterogeneous study settings, identifies key drivers in a multivariate framework, and transparently documents areas of dense versus sparse evidence. This meta-analysis addresses these gaps by harmonizing 146 studies (917 observations) into a common effect size (DegRate). We estimate multivariate moderator effects in a meta-regression framework to quantify how key moderators shape degradation across battery differences, experimental characteristics, measurement characteristics, and publication characteristics. We also apply Bayesian model averaging to quantify moderator importance and posterior effect estimates under model uncertainty. Beyond confirming established qualitative insights, we provide descriptive quantitative degradation benchmarks. In addition, we use the estimated moderator effects to generate model-implied scenario estimates of DegRate across experimental settings, including combinations that are only partially represented in the literature. Where evidence is limited, we reflect this explicitly in wider uncertainty intervals, and the resulting heatmaps, which visualize evidence density across experimental regimes, highlight priorities for future experimental work.

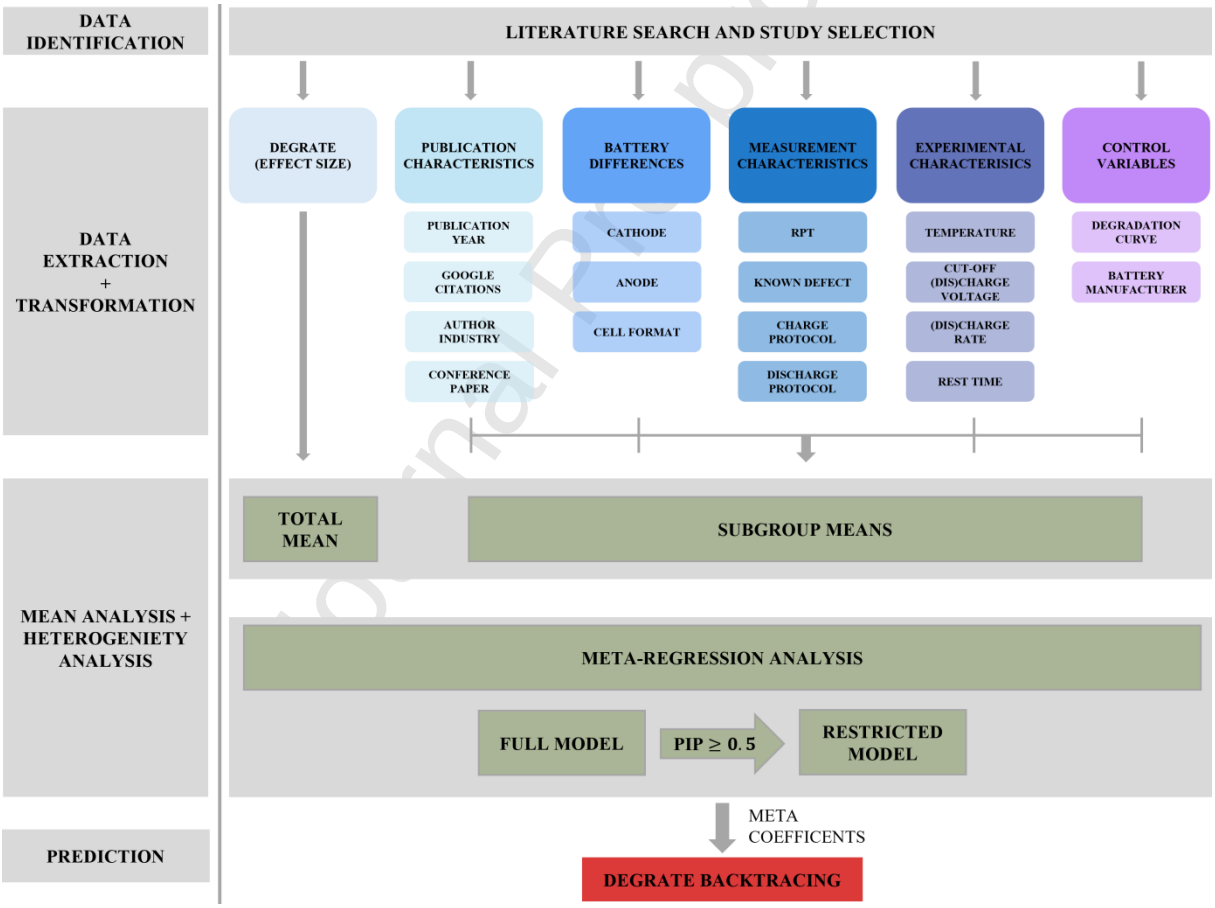

Figure 1: Overview of the meta-analysis framework on the degradation of LIBs.

2 Methodology

2.1 Literature Search

To examine the aggregated effect of reported DegRates of LIBs and the factors contributing to its heterogeneity within and across studies, we constructed a meta-data set through a string-based keyword search of scientific literature using Google Scholar on April 20, 2024**,** in accordance with the

established guideline for meta-analysis [33]. We developed the search string using the PICO **(**Population, Intervention, Comparison, and Outcomes**)** framework introduced by Richardson et al. [34]. We applied its extended form, PICOS, which includes study design, as recommended by Campbell Collaboration [35] (Table S1). The framework was implemented through an iterative process, in which successive versions of the search string were tested and refined. The string was narrowed when the results predominantly included irrelevant studies and broadened when important studies were missing. The final dataset comprised 2**,**210 studies, of which 239 were identified as duplicates**.**

A uniform effect size is the key input for meta-analysis. Following the literature, we define the DegRate as a capacity loss leading to 80 % of the initial capacity as a function of the number of charge-discharge cycles [4,36,37]. Conceptually, DegRate is an interval-averaged measure of capacity fade per cycle until the capacity declines to 80% of its initial value. Therefore, DegRate is an end-of-life benchmark, not a local slope at a specific cycle number, and it does not identify underlying degradation mechanisms on its own. While degradation trajectories may differ, they are comparable in terms of the average fade required to reach a common end-of-life threshold, which is particularly useful, given that studies report capacity trajectories at different temporal resolutions and levels of detail. If a battery's end-of-life (EoL) threshold was not reached due to exceptionally high cycle stability, the DegRate was calculated based on the slope of the capacity degradation curve up to the last reported cycle, similar to the approach of Dechent et al. [9]. When the DegRate was presented only in graphical form, we manually extracted the values using WebPlotDigitizer (version 5.0, https://automeris.io/WebPlotDigitizer). To account for systematic differences, we explicitly coded the shape of the degradation trajectory and statistically controlled for it in the meta-regression analysis.

During the full-text screening process, we considered only studies that met the following criteria: (i) Studies had to report the DegRate of LIBs as defined above. (ii) We excluded studies focusing solely on half cells, as full-cell configurations provide a more practical assessment of degradation by capturing the realistic interaction between the anode and cathode. (iii) Studies had to examine the LIB experimentally using cycle tests (reviews and other secondary literature were excluded). (iv) In addition, we excluded studies that report degradation per full equivalent cycle rather than per individual charge-discharge cycle, as the two metrics are not directly comparable. (v) Studies focusing on battery packs were also excluded, since pack-level degradation can be influenced by interconnection effects that do not reflect cell-level behavior. The systematic literature screening process, as illustrated in the PRISMA flowchart (Figure S2), resulted in a final dataset of 146 primary studies (Table S2), most of which reported multiple DegRate observations, totaling 917 data points. This dataset forms the basis for the descriptive analyses presented in Section 3.1.

2.2 Dataset Construction

We conducted an in-depth analysis of the full texts and supplementary materials to extract potential moderators determining the differences in reported DegRate observations. In total, we identified 67

moderator variables spanning both numerical and categorical variables. We excluded moderators with substantial missing numerical data, such as experimental duration, battery mass, and electrolyte composition. Similarly, we omitted depth of discharge and state of charge, as most studies defined the operating window through charge and discharge cut-off voltages rather than reporting these values directly. The full dataset of 146 studies and 917 observations was used for descriptive analyses, providing the most comprehensive representation of reported degradation behavior. The identified moderators can be classified into five main categories: publication characteristics, battery differences, measurement characteristics, experimental characteristics, and control variables. We included publication characteristics, such as the number of Google Scholar citations per year, to test whether more frequently cited papers tend to report more extreme effect sizes. Battery differences address electrode chemistry and cell format, as these factors may influence degradation outcomes systematically. Measurement characteristics cover aspects such as the applied charge–discharge protocol, and whether known defects were revealed by the analysis before or after the experiment. Known defects are defined as visible or measurable degradation mechanisms that are consistently addressed in review studies [3–5,38]. Experimental characteristics describe the operational conditions during cycling, such as the temperature settings and the charge cut-off voltages. Finally, control variables capture the shape of the degradation trajectory (linear, decelerated, or accelerated) [39] and examine whether DegRate was affected by the battery's origin from a specific manufacturer. The final set of categories, along with study *n* and observation *m* counts, is summarized in Table 1. For regression analyses, sparsely represented categorical moderators were merged into broader groups to ensure sufficient representation, statistical validity, and comparability.

Table 1: Variable description

Variable	Description	Mean	Std. Dev.	n (m)
Battery differences				
CATHODE: LFP	=1, if the cathode is LFP	0.160	0.367	27 (142)
CATHODE: LCO	=1, if the cathode is CO	0.102	0.303	16 (91)
CATHODE: NCA	=1, if the cathode is NCA	0.057	0.233	14 (51)
CATHODE: NMC*	=1, if the cathode is NMC	0.550	0.498	75 (488)
CATHODE: LMO	=1, if the cathode is LMO	0.020	0.141	6 (18)
CATHODE: LNMO	=1, if the cathode is LNMO	0.020	0.141	5 (18)
CATHODE: NMC+NCA	=1, if the cathode is NMC+NCA	0.027	0.162	3 (24)
CATHODE: NCA+LNO	=1, if the cathode is NCA+LNO	0.021	0.145	1 (19)
CATHODE: LNCO	=1, if the cathode is LNCO	0.007	0.082	1 (6)
CATHODE: LNO	=1, if the cathode is LNO	0.005	0.067	1 (4)
CATHODE: NCA+LMO	=1, if the cathode is NCA+LMO	0.005	0.067	1 (4)
CATHODE: NMC+LMO	=1, if the cathode is NMC+LMO	0.026	0.159	6 (23)
ANODE: SI-BASED	=1, if the anode contains silicon	0.084	0.277	11 (70)
ANODE: GRAPHITE*	=1, if the anode is graphite	0.810	0.392	103 (679)
ANODE: MCMB	=1, if the anode is MCMB	0.057	0.233	9 (48)
ANODE: LTO	=1, if the anode is LTO	0.031	0.173	6 (26)
ANODE: OTHER CARBON	=1, if the anode is made of any other type of carbon	0.018	0.133	5 (15)
FORMAT: COIN CELL	=1, if the Battery is a coin cell	0.125	0.331	20 (106)
FORMAT: POUCH CELL	=1, if the Battery is a pouch cell	0.377	0.485	41 (319)

FORMAT: PRISMATIC CELL	=1, if the Battery is a prismatic cell	0.071	0.257	11 (60)
FORMAT: CYLINDRICAL CELL*	=1, if the Battery is a cylindrical cell	0.427	0.495	63 (362)
Measurement characteristics				
MEASUREMENT: RPT	=1, if the capacity was determined by RPT	0.439	0.497	57 (401)
MEASUREMENT: KNOWN DEFECT	=1, if the study reports any known defect	0.456	0.498	75 (413)
MEASUREMENT: CV CHARGE PROTOCOL	=1, if a constant voltage protocol was used	0.747	0.435	95 (677)
MEASUREMENT: CONSTANT DISCHARGE PROTOCOL	=1, if a constant discharge protocol was used	0.945	0.228	132 (860)
Experimental characteristics				
EXPERIMENT: TEMPERATURE	Temperature of the experiment in °C	26.487	17.055	126 (833)
EXPERIMENT: TEMPERATURE COLD	=1, if the temperature is below 0 °C	0.082	0.274	10 (68)
EXPERIMENT: TEMPERATURE LOW	=1, if the temperature is between 0 °C and 20 °C	0.066	0.248	16 (55)
EXPERIMENT: TEMPERATURE WARM	=1, if the temperature is between 20 °C and 40 °C	0.606	0.489	103 (505)
EXPERIMENT: TEMPERATURE HOT	=1, if the temperature is 40 °C or above	0.246	0.431	41 (205)
EXPERIMENT: CUT-OFF CHARGE VOLTAGE	Charge cut-off voltage of the experiment	4.127	0.352	133 (859)
EXPERIMENT: CUT-OFF DISCHARGE VOLTAGE	Discharge cut-off voltage of the experiment	2.659	0.504	129 (828)
EXPERIMENT: OVERCHARGED	=1, if the Battery is overcharged	0.058	0.234	5 (53)
EXPERIMENT: OVERDISCHARGED	=1, if the Battery is overdischarged	0.026	0.160	4 (24)
EXPERIMENT: STANDARD CHARGE/DISCHARGE	=1, if the Battery undergoes standard (dis)charge cycles	0.916	0.278	140 (838)
EXPERIMENT: CHARGE RATE	Charge rate of the experiment	0.980	0.986	138 (861)
EXPERIMENT: DISCHARGE RATE	Discharge rate of the experiment	1.542	5.246	138 (881)
EXPERIMENT: REST TIME	=1, if there is a rest time between charging and discharging	0.292	0.455	51 (263)
Control variables				
CONTROL: DECELERATED	=1, if the degradation curve has a decelerating shape	0.408	0.492	68 (366)
CONTROL: ACCELERATED	=1, if the degradation curve has an accelerated shape	0.238	0.426	58 (214)
CONTROL: LINEAR*	=1, if the degradation curve has a linear shape	0.354	0.479	89 (318)
CONTROL: BATTERY MANUFACTURER	=1, if the battery manufacturer is known	0.638	0.481	90 (585)
Publication characteristics				
PUBLICATION: YEAR	Publication year of the study	2020.213	2.989	146 (917)
PUBLICATION: GOOGLECITS	Google citations per study	52.568	121.582	146 (917)
PUBLICATION: AUTHOR INDUSTRY	=1, if one author has a connection to the industry	0.262	0.440	34 (240)
PUBLICATION: CONFERENCE PAPER	=1, if the paper is a conference paper	0.085	0.279	13 (78)

*Notes: This table presents the definition and summary statistics of the variables included in the meta-analysis based on n = 146 studies and m = 917 observations. Dummy variables are coded 0/1; their means equal sample shares. * marks the omitted baseline category in each N–1 related dummy set used in the meta-regression.*

To enhance interpretability and reduce redundancy, highly correlated moderators were either simplified or omitted. For instance, rest time after charge or discharge was simplified to a binary indicator, while cathode structure was excluded due to its strong correlation with cathode material.

Variance inflation factors (VIF) were then calculated and found to be well below the conventional threshold of 5 [40], confirming that multicollinearity is not a concern in the meta-regression models. To improve the model's fit and reduce bias, selected continuous moderators were transformed using the natural logarithm. Specifically, the publication year was transformed relative to the earliest year in the dataset to ensure comparability over time. Rather than including total citation counts, which would disproportionately favor older studies, log-transformed annualized Google Scholar citations per study were used to account for differences in publication age, following established best practice [41–44]. In addition, the charge rate, discharge rate and charge and discharge cut-off voltages were all log-transformed to reduce the influence of extreme values and ensure a more balanced representation across their wide ranges. Because of these adjustments and inconsistent moderator reporting across primary studies, the dataset for regression-based analysis was restricted to cases without missing values. This resulted in a final dataset of 88 studies and 627 observations.

2.3 Meta-regression Analysis and Bayesian Model Averaging

The large design space in battery-aging studies, driven by variations in experimental, measurement, and battery-specific factors, introduces substantial heterogeneity, resulting in considerable variability in reported DegRates. To disentangle the contributions of each moderator, we estimate a single-model meta-regression (MRA), following Stanley and Jarrel [45], that provides direct coefficient estimates, quantifying their average impact on DegRate (Eq. (3)). Each coefficient reflects the change in mean DegRate, expressed in percentage points per cycle, associated with a one-unit increase in the respective moderator.

$$DegRate_{mn} = \alpha + \sum_{k=1}^{K} \beta_k Z_{mnk} + \varepsilon_{mn} \quad (3)$$

$DegRate_{mn}$ represents the DegRate of the m-th estimate from the n-th study, β_k are the meta-regression coefficients, Z_{mnk} signifies the set of K moderator variables, and ε_{mn} is the error term. Since multiple observations are often reported within the same primary study, we clustered robust standard errors at the study level to account for within-study dependencies. This common practice mitigates undue influence from studies with many estimates and ensures a more balanced synthesis of the evidence [15,46].

We also follow an established approach in meta-analysis and employed Bayesian model averaging (BMA) to address model uncertainty and to analyze the simultaneous influence of multiple moderators on DegRate [19,47–51]. The fundamental idea of BMA is to estimate a large set of meta-regression models, each representing a different subset of moderators. This would involve estimating 2^K possible regression specifications, where K is the number of explanatory variables in the meta-regression. Because estimating all possible model specifications would be substantial resource-intensive, we employed Markov Chain Monte Carlo Model Composition. This algorithm efficiently samples the model space by prioritizing specifications with higher posterior model probabilities (PMP), thereby

reducing the computational burden while maintaining statistical rigor. The PMP quantifies the explanatory power of each model specification and is conceptually similar to the adjusted R^2 in classical regression analysis. By averaging over all sampled models, BMA produces posterior inclusion probabilities (PIP) for each moderator. The PIP ranges between 0 and 1, representing the likelihood that a moderator belongs in the true degradation model [52]. To account for potential collinearity among moderators, we applied a dilution prior, as proposed by George [53]. This assigns lower weight to models with highly correlated predictors due to lower determinant of their correlation matrix. Additionally, we implemented unit-information g-prior, which assumes that the prior information corresponds to that of a single observation [54]. Furthermore, BMA provides posterior means (Post Mean) that describe the magnitude and direction of the effect, along with corresponding posterior standard deviations (Post SD) that represent the associated uncertainty. Based on the PIP derived from BMA, we also restricted the single-model meta-regression, excluding moderators with little or misleading explanatory power.

A methodological challenge arises from the fact that primary studies on battery degradation rarely report standard errors of their effect sizes. In conventional meta-regression, such information is necessary to construct weighted least squares (WLS) regressions, assigning greater weight to more precise studies [18]. Since our meta-dataset comprises experimentally observed DegRate rather than statistical estimates, and because, to the best of our knowledge, this is the first meta-analysis of LIB degradation, we present baseline results from unweighted MRA. Nevertheless, we provide robust results using WLS meta-regressions, applying two alternative weighting schemes in place of standard errors to control potential heteroscedasticity in the regression residuals. The first model (WLS1) applies inverse weights based on the number of observations per study, an established approach in meta-analysis research [55], preventing studies with disproportionately many data points from influencing the results. WLS1 is simple and transparent, however it does not account for differences in study quality or measurement reliability beyond the number of reported observations. The second model (WLS2) relies on a custom study-quality index that penalizes the lack of key methodological details or the failure to reach the EoL threshold of 80 % each resulting in a two-point penalty, while missing information on the tested battery incurred a one-point penalty [19]. In total, studies could accumulate up to 15 penalty points, with higher scores indicating lower reliability (Table S8). We then transformed the penalty score into a continuous quality measure using 1/(1+penalty), producing a normalized index where values approaching 1 indicate higher-quality studies. WLS2 reflects heterogeneity in reporting completeness and methodological rigor, which would otherwise be treated equally in an unweighted specification. However, since the index is self-constructed, it necessarily involves subjective design choices. Finally, the estimated coefficients enable us to create hypothetical study scenarios by assigning specific values to moderators. These scenarios provide model-implied benchmark estimates of expected degradation outcomes under given conditions, thereby illustrating the practical impact of moderators on DegRate.

3 Results and Discussion

This section presents the core findings of the meta-analysis on LIB degradation. Drawing on our dataset of 146 primary studies we identify key patterns, sources of variability, and trends in degradation behavior. The results offer a quantitative foundation for understanding how various experimental and design factors influence battery performance over time.

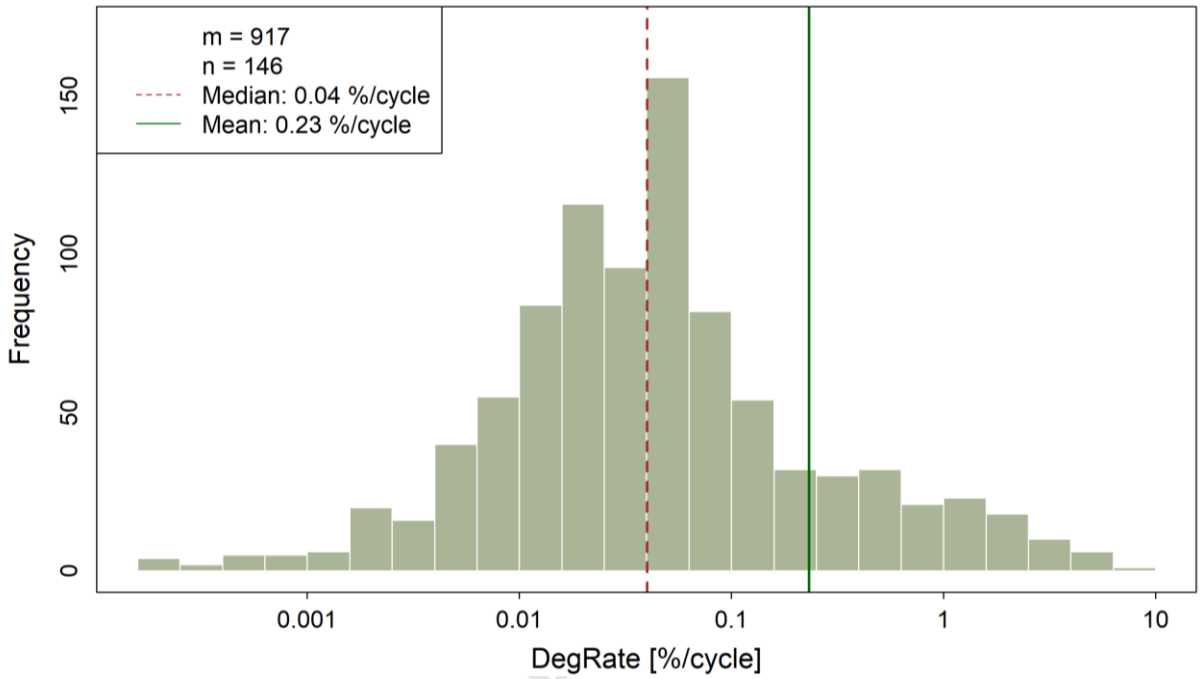

Figure 2: Histogram of reported DegRate across all included 146 studies (n) and 917 observations (m). The x-axis is displayed on a logarithmic scale to accommodate the wide range of reported values. The solid green indicates the arithmetic mean (0.23 %/cycle), while the dashed red line represents the median (0.04 %/cycle) of the whole sample.

The distribution of DegRate exhibits a pronounced right-skewed shape (Figure 2). The median DegRate of our full sample of 146 studies and 917 observations is 0.04 %/cycle, while the mean is 0.23 %/cycle. The values observed range from nearly 0 % to about 8 %/cycle, highlighting the considerable heterogeneity within the dataset and the need for comprehensive meta-analysis to explore the drivers of this variability.[1] In terms of cell origin, 503 of the 917 observations (87 studies) are based on commercial cells, 306 observations (43 studies) on non-commercial cells, and the remaining 108 observations (22 studies) lack sufficient reporting for classification. A more granular categorization of the non-commercial group (e.g., lab-scale vs. pilot-line prototypes) was not feasible because such information is rarely reported in the primary literature. To increase transparency, we coded studies by investigating either high-power or high-energy batteries when this information was available in the primary sources. Among the 146 studies (917 observations), 26 (198 observations) were classified as high-energy, and 25 (124 observations) were classified as high-power. The remaining studies were unclear because of insufficient reporting. Due to sparse coverage, we could not consider these variables further in our analysis. The large variation of DegRate suggests that numerous

[1] This observation is further supported by Figure S3, which exemplifies the distribution of DegRate based on a subset of 47 Studies.

study-specific aspects play a significant role in influencing degradation behavior, including experimental characteristics, measurement characteristics, and battery differences. The strength of the evidence depends not only on the quality of the underlying experimental data, but also on the number of observations available for a given combination of moderators. While individual studies may rely on robust experimental methods, limited data density reduces statistical power and constrains the generalizability of effect estimates. Consequently, results based on a small number of observations or studies should be interpreted with caution. Nevertheless, these cases are reported because they highlight underexplored regimes and help identify research gaps. In the following sections, we examine which specific factors of data and study design are associated with higher or lower DegRate.

3.1 Univariate Meta-Analysis

The univariate analysis is based on the full sample ensuring the most comprehensive coverage of reported DegRate. This allows for an initial investigation of potential influencing factors prior to the extensive data harmonization required for the regression models (e.g., merging sparse categories, simplifying correlated moderators, and applying transformations), which reduces the number of observations for the analysis. To systematically investigate the observed heterogeneity in DegRate, we examined both experimental parameters (such as temperature and voltage range) and battery differences (including anode and cathode materials, as well as cell format). Figure 3 summarizes these effects by displaying the mean DegRate and their 95 % confidence intervals for all the main moderator categories and their subgroups. The number of studies *n* and observations *m* underlying each estimate is reported, and subgroup means are further aggregated when they share common characteristics.

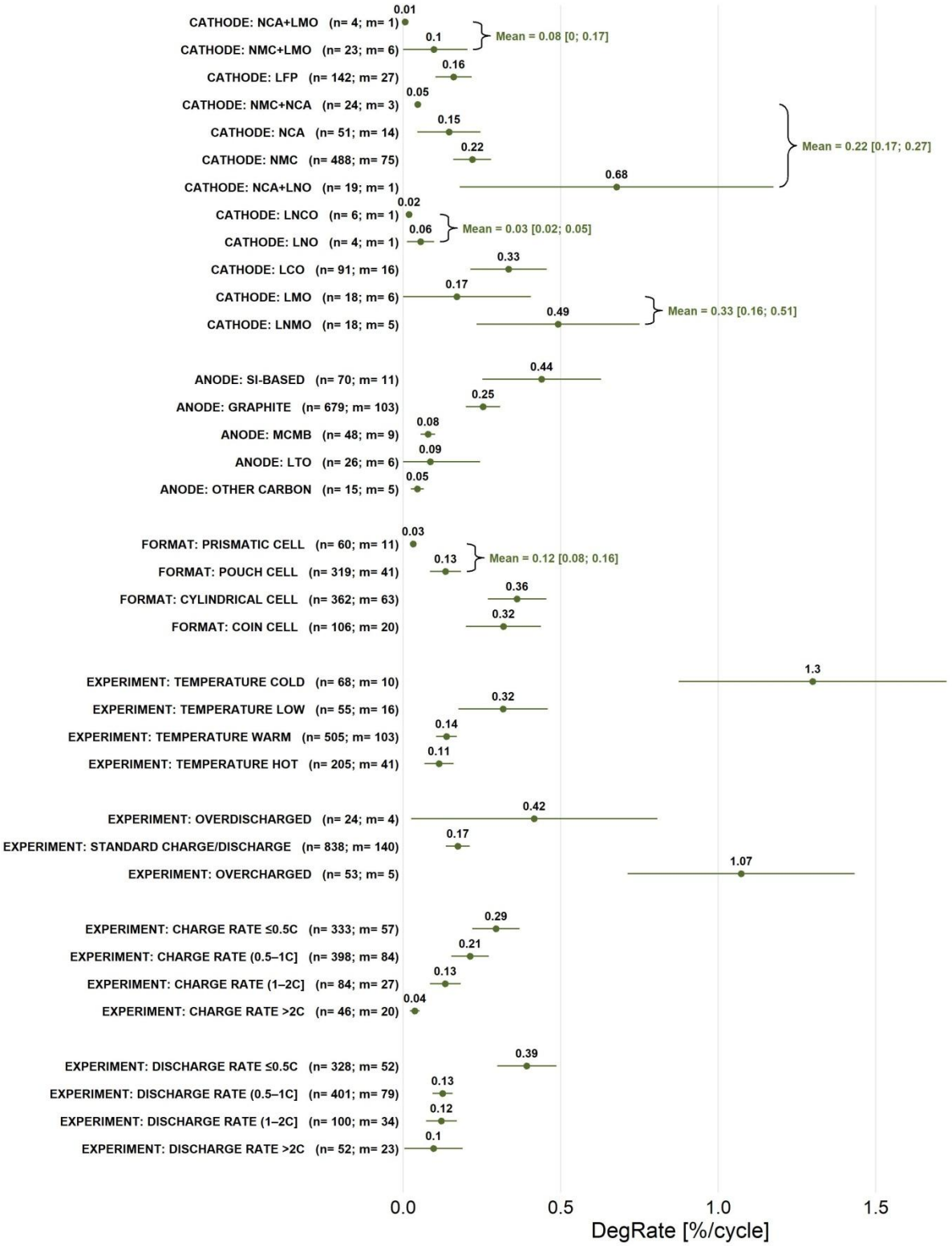

Figure 3: The mean DegRate are shown for the following subcategories: cathode, anode, cell format, temperature, voltage conditions, and C-rates (charge and discharge rates). Temperature categories are defined as follows: cold <0 °C, low [0 – 20 °C), warm [20–40 °C), and hot ≥40 °C. Charge and discharge rates are grouped as follows: ≤0.5C, (0.5–1C], (1 – 2C], and >2C. The points represent the means of the subgroups, and the horizontal lines indicate the 95 % confidence intervals. Curly brackets group subcategories with common characteristics, and the corresponding aggregated mean values with confidence intervals are displayed on the right. The number of studies n and observations m for each subcategory in the whole sample of 146 studies and 917 observations are shown on the left and the CI lower boundary is truncated at zero. For full results, see Table S3.

A key result emerges from comparing cathode materials, revealing clear differences in mean DegRate and its 95 % confidence intervals. LFP cathodes do not exhibit exceptionally low values, contradicting

the common assumption of their superior cycle stability, with a mean of 0.16 [0.10; 0.22] %/cycle [4,56]. However, Black et al. [57] show that LFP cells can undergo markedly accelerated aging at elevated temperatures, and Azam et al. [58] further report inferior high-temperature cycling performance for LFP compared with NMC under comparable conditions. NMC- and NCA-based cathodes have an average of 0.22 [0.17; 0.27] %/cycle but show substantial internal variation, partly driven by varying sample sizes. This is consistent with known structural degradation pathways of nickel-rich layered oxides, where delithiation-induced phase transitions and oxygen release can increase resistance growth and cycling instability. LCO cathodes show comparatively higher aging, with a mean of 0.33 [0.21; 0.46] %/cycle, which could indicate a reduced service life. This may reflect intrinsic cycle life limitations or the fact that this well-studied material is probably often tested under harsher or more demanding conditions nowadays, which can amplify DegRate [59,60]. Mixed chemistries, such as NCA+LMO and NMC+LMO, are among the lowest at 0.08 [0; 0.17] %/cycle, which may indicate synergistic stability benefits. Interpretation, however, is limited by the small sample size.

Clear differences in DegRate central tendency are also observed across the various anode groups. Graphite is by far the most frequently studied anode material (n = 679, m = 103) and is a well-established technology often used as a benchmark. Its mean DegRate of 0.25 [0.20; 0.31] %/cycle is relatively high; although graphite is known for its cycle stability, the elevated DegRate observed in some studies is likely due to testing under more extreme conditions, which can promote SEI growth, structural disordering, and lithium plating. MCMB (mesocarbon microbeads), a synthetic form of graphite, shows a lower mean of 0.08 [0.06; 0.10] %/cycle. The reduced DegRate can be attributed to their high rate capability and good cycle performance, albeit at higher production cost [61,62]. In contrast, silicon-based anodes exhibit a higher mean of 0.44 [0.25; 0.63] %/cycle with a markedly wider spread, consistent with well-known challenges such as volume expansion and structural instability during cycling [3,63,64]. LTO anodes show a relatively low mean of 0.09 [0.00; 0.24] %/cycle, in line with previous findings that attribute this stability to structural advantages such as a stable spinel lattice and minimal SEI formation and avoidance of dendrite formation, ensuring high safety [30,65,66]. However, the small sample size (n = 6, m = 26) limits the generalizability of this result. The low DegRate tendency for LTO anodes is qualitatively consistent with Dechent et al. [9] who found that LTO-based cells have an exceptionally long lifetime. However, a direct quantitative comparison is not feasible because their metric for lifetime is based on energy throughput and full equivalent cycle.

Moreover, DegRate varies considerably by cell format. Coin cells, primarily used in materials research, exhibit a high mean of 0.32 [0.20; 0.44] %/cycle, similar to cylindrical cells mainly used by Tesla [67–69]. In contrast, rectangular formats, such as pouch and prismatic cells, show notably lower DegRate, with a shared mean of 0.12 [0.08; 0.16] %/cycle. These formats are widely adopted in practical applications, particularly in the automotive and consumer sectors. Han et al. [4] attribute the

lower DegRate of rectangular cells to their favorable thermal properties. Cylindrical cells have a smaller specific surface area and therefore dissipate heat less efficiently, resulting in higher internal temperatures. In contrast, prismatic and pouch cells benefit from their large external surface areas, which enable efficient heat dissipation and more uniform temperature distribution. Similarly, Saber et al. [70] emphasize that prismatic cells are well-suited for efficient thermal management due to their large specific surface area, which promotes uniform thermal conditions. Beyond thermal considerations, Han et al. [4] highlight mechanical factors as well. Pouch and prismatic cells generally experience lower, more evenly distributed mechanical stresses than cylindrical cells, a difference most pronounced in prismatic designs. Cylindrical cells, by contrast, contain a tightly wound electrode assembly that increases stress heterogeneity and reduces the electrolyte inventory. Consequently, electrolyte depletion caused by lithium plating can lead to more pronounced capacity fading. Additionally, the dynamic bending of electrodes inherent to the cylindrical winding process produces inhomogeneous mechanical forces that accelerate aging [71]. Beyond these format-specific factors, differences in observed degradation may also be influenced by experimental conditions. Our dataset shows that cylindrical cells are by far the most frequently studied cell format. This prevalence likely reflects their high degree of standardization, which makes them comparable across studies [72]. However, because academic research often relies on accelerated aging protocols under harsh operating conditions, these practices may reinforce the perception that cylindrical cells degrade more quickly than prismatic or pouch cells. Finally, coin cells are primarily used in materials research, where they typically serve as test carriers for immature or unoptimized chemical compositions [73,74]. This exploratory use may partly explain the comparatively higher DegRates often reported for this format.

The analysis shows significant variation in the central tendency of DegRate as a function of operating temperature. At temperatures below 0 °C (Cold), the mean DegRate reaches 1.30 [0.87; 1.72] %/cycle, highlighting the well-documented challenges of cold-temperature operation. These include increased electrolyte viscosity, reduced lithium-ion mobility, and a heightened risk of lithium plating [75–79]. In contrast, at moderate to elevated temperatures, the DegRates are comparatively low. This result is particularly notable, as high temperatures are often linked to accelerated degradation in literature [7,80,81]. One possible explanation for the lower DegRates under hot conditions could be the use of adapted testing strategies, such as optimized cell chemistries or effective thermal management systems.

The analysis of different voltage conditions reveals pronounced differences in the mean DegRate. Most notably, under overcharged conditions, the DegRate rises sharply to a mean of 1.07 [0.71; 1.43] %/cycle. This aligns with well-established electrochemical mechanisms: overcharging induces electrolyte decomposition, side reactions at the cathode, and lithium plating [4,82]. In contrast, overdischarging results in a modest increase, with a mean of 0.42 [0.03; 0.81] %/cycle compared to 0.17 [0.14; 0.21] %/cycle under standard operation. This finding is somewhat unexpected, as deep discharge is associated with harmful side reactions, such as copper dissolution from the current

collector and SEI breakdown [83,84]. A possible explanation may lie in the conservative interpretation of voltage limits or that the overdischarge tests were less aggressive than overcharge protocols. However, our results are corroborated by the findings of Ouyang et al. (2019) [85]. They also identified overcharging as having a greater influence on the DegRate than overdischarging. It should also be noted that the overcharged group is based on only five studies, therefore, the results must be interpreted with caution. Nonetheless, they provide a strong indication of the substantial damage potential associated with excessive charging voltages.

In battery aging literature, higher C-rates (charge and discharge rates) are commonly treated as stressors and are often associated with accelerated degradation [3,5,86]. However, Ouyang et al. [87] demonstrate that the apparent C-rate effect depends on the operating regime (e.g., temperature) and on whether degradation is evaluated per cycle or per unit time, because lower C-rates imply longer cycle durations and may therefore accumulate more time-dependent aging per cycle. Consistent with this, the descriptive subgroup means in Figure 3 do not show a monotonic increase in DegRate with increasing C-rate. Instead, higher charge rates tend to be associated with lower mean DegRate, while discharge rates show no consistently monotonic pattern, with the lowest discharge-rate category exhibiting the highest mean DegRate. One plausible explanation is the confounding effect of other experimental choices, notably temperature and voltage window, together with regime-dependent mechanism shifts (e.g., SEI growth vs. lithium deposition). In particular, the crossover between these regimes has been reported to shift with C-rate [88]. Gao et al. [79] report a temperature-charge rate map of expected cycle life and discuss operating conditions in which lower charge rates can exhibit shorter cycle life than higher charge rates due to longer single-cycle times and SEI-related lithium loss, while high charge rates remain detrimental at low temperatures due to lithium plating.

3.2 Multivariate Modeling of Degradation Drivers

While subgroup analysis examines moderators individually, our multivariate analysis aims to identify the drivers of DegRate simultaneously, helping to address the potential bias introduced when factors are evaluated in isolation. Table 2 presents the results from BMA and unweighted MRA based on the dataset consisting of 88 studies, providing the core quantitative findings in the main text (dominant moderators and their effect magnitudes), evaluating the impact of publication characteristics, battery differences, measurement characteristics, and experimental characteristics on DegRate in LIBs. The BMA results are summarized through PIP, posterior means and their standard deviations, while the MRA columns report conventional regression coefficients, once for the full set of moderators, once restricted to the standard of PIP $\geq$ 0.50, and a stricter model with a threshold at PIP $\geq$ 0.65 [89]. The purpose of the restriction is to eliminate variables with less explanatory power from the model, thus enhancing the accuracy and stability of the estimates [90]. Meta-regression coefficients quantify conditional mean differences in DegRate relative to the base category, or per-unit changes for continuous moderators. For instance, a constant-voltage (CV) charging protocol is associated with a 0.258 percentage point lower DegRate compared to other charging methods, holding all other

moderators constant.[2] Additionally, the BMA results are illustrated in Figure S4, while Table S7 reports meta-regressions with alternative weighting schemes as robustness checks. Across specifications, the main drivers of DegRate, supported by consistently high PIPs and unweighted meta-regression estimates, are temperature, a decelerated degradation trajectory, the presence of a defect, the upper cut-off voltage, and the availability of manufacturer information.

Table 2: BMA and MRA main results

	Bayesian model averaging			Unweighted meta-regression		
Moderator variable	Post Mean	Post SD	PIP	ALL-UW	0.50-UW	0.65-UW
INTERCEPT	-1.553	-	1.000	-0.829 (-0.796)	-1.906** (-2.596)	-2.397*** (-2.821)
Battery differences						
CATHODE: LFP[1]	-0.148	0.150	0.555	-0.294 (-0.894)	-0.261 (-1.208)	-
CATHODE: LCO[1]	<0.001	0.014	0.023	-0.026 (-0.112)	-0.101 (-0.637)	-
CATHODE: NCA[1]	-0.002	0.022	0.026	-0.137 (-0.646)	-0.103 (-0.686)	-
CATHODE: OTHER[1]	<0.001	0.011	0.021	-0.065 (-0.380)	-0.029 (-0.198)	-
ANODE: SI-BASED[2]	0.182	0.146	0.675	0.266 (1.467)	0.293 (1.607)	0.313* (1.768)
ANODE: OTHER[2]	0.007	0.038	0.054	0.142 (0.817)	0.111 (0.918)	0.136 (1.239)
FORMAT: COIN CELL[3]	-0.001	0.018	0.029	-0.060 (-0.311)	-	-
FORMAT: POUCH CELL[3]	0.006	0.028	0.063	0.057 (0.397)	-	-
FORMAT: PRISMATIC CELL[3]	-0.050	0.118	0.185	-0.436 (-1.672)	-	-
Measurement characteristics						
MEASUREMENT: RPT	0.003	0.019	0.036	0.123 (0.838)	-	-
MEASUREMENT: KNOWN DEFECT	0.331	0.058	1.000	0.257*** (2.966)	0.331*** (3.144)	0.324*** (3.317)
MEASUREMENT: CV CHARGE PROTOCOL	-0.090	0.103	0.492	-0.258*** (-2.722)	-	-
MEASUREMENT: CONSTANT DISCHARGE PROTOCOL	0.001	0.025	0.020	0.137 (0.618)	-	-
Experimental characteristics						
EXPERIMENT: TEMPERATURE	-0.015	0.002	1.000	-0.014*** (-3.403)	-0.015*** (-3.063)	-0.014*** (3.359)
EXPERIMENT: CUT-OFF CHARGE VOLTAGE	1.586	0.338	1.000	1.490* (1.930)	1.881*** (3.049)	2.151*** (3.286)
EXPERIMENT: CUT-OFF DISCHARGE VOLTAGE	-0.075	0.109	0.370	-0.255 (-0.722)	-0.244 (-0.737)	-0.209 (-0.654)
EXPERIMENT: CHARGE RATE	-0.001	0.009	0.037	-0.017 (-0.157)	-	-
EXPERIMENT: DISCHARGE RATE	-0.001	0.007	0.028	-0.042 (-0.488)	-	-
EXPERIMENT: REST TIME	<0.001	0.010	0.022	0.013 (0.096)	-	-
Control variables						
CONTROL: DECELERATED[4]	0.305	0.059	1.000	0.355* (1.798)	0.332* (1.987)	0.317* (1.959)
CONTROL: ACCELERATED[4]	0.066	0.098	0.356	0.185 (1.266)	0.103 (0.831)	0.122 (0.965)
CONTROL: BATTERY MANUFACTURER	-0.269	0.060	0.999	-0.347** (-2.605)	-0.250** (-2.037)	-0.256** (-2.241)
Publication characteristics						
PUBLICATION: YEAR	-0.001	0.016	0.026	-0.147 (-0.960)	-	-
PUBLICATION: GOOGLECITS	-0.001	0.065	0.020	-0.769 (-1.204)	-	-
PUBLICATION: AUTHOR INDUSTRY	-0.052	0.081	0.338	-0.100 (-0.944)	-	-
PUBLICATION: CONFERENCE PAPER	-0.001	0.017	0.023	-0.002 (-0.011)	-	-
Studies (observations)		88 (627)		88 (627)	88 (627)	88 (627)
R^2 *(adjusted)*	-	-	-	0.337	0.319	0.315

Notes: The table reports the main quantitative results from Bayesian model averaging (BMA) and the baseline unweighted

[2] For moderators modeled in logarithmic form, coefficients reflect proportional rather than one-unit changes. For example, increasing cut-off charge voltage from V_1 to V_2 implies an expected change of $\beta \cdot ln(V_2/V_1)$ percentage points in DegRate, holding all other moderators constant.

meta-regressions. The dependent variable across all models is the degradation rate (DegRate). BMA condenses its findings into posterior inclusion probabilities (PIPs). A higher PIP indicates that a given moderator is selected in a larger share of the regression specification in the BMA. The posterior mean (Post mean) shows the direction and average magnitude of each moderator's effect, while the posterior standard deviation (Post SD) quantifies the associated uncertainty. The right-hand panel presents three columns of unweighted meta-regression estimates (UW): the first reports coefficients for the complete set of moderators (ALL-UW), whereas the second combines all variables with a PIP ≥ 0.50 (0.50-UW). The third one retains only those moderators whose PIP ≥ 0.65 (0.65-UW). For example, in the meta-regression column that includes all moderators, the coefficient of −0.258 indicates that studies examining batteries charged with a constant voltage (CV) protocol report DegRates that are on average 0.258 percentage points lower than other charging methods. The t-statistics are reported in parentheses. The significance level for 0.1, 0.05, 0.01 corresponds to "", "**" and "***" respectively. The base categories for the dummy variables were chosen as the most frequently observed specifications: [1]NMC, [2]graphite, [3]cylindrical cell, and [4]linear degradation trajectory. Meta-regressions using alternative weighting schemes are reported as robustness checks in Table S7.*

The BMA results, presented alongside the classical MRA estimates, reveal several key patterns. The temperature variable exhibits the highest possible PIP (1.000) and a strong, statistically significant negative effect in the meta-regression, consistent with findings from previous studies [75–79]. A robustness analysis that replaces the continuous temperature variable with temperature bins using the Figure 3 cut points is reported in the Supplementary Material (S.9). Similarly, high charge cut-off voltage has a PIP of 1.000 and a consistently large, significant MRA coefficient (1.490 percentage points). In both the PIP ≥ 0.50 model and PIP ≥ 0.65 specification, the effect becomes even more statistically robust with coefficients of 1.881 percentage points and 2.151 percentage points, respectively, confirming its critical role in accelerating battery degradation and in line with existing literature [91–93]. As expected, an observed or measured defect leads to a significant increase in DegRate. Finally, the negative coefficient of the battery manufacturer suggests that cells from established manufacturers are more technologically mature and therefore less prone to extreme degradation. We focus on battery manufacturers as a reproducible proxy for commercial cell provenance. This is because commercial status is often not explicitly stated and would require additional inference, and finer distinctions (e.g. lab-scale vs. pilot-line prototypes) are rarely reported consistently in primary literature. This negative coefficient may also reflect a possible publication selection bias, where studies using branded cells are more likely to be published when performance is favorable. Publication bias refers to the tendency of researchers, journal editors, or peer reviewers to preferentially submit or accept studies reporting statistically significant, novel, or large effect sizes, leading to the suppression of insignificant or contrary findings [18,94,95].

The cathode materials show limited incremental contribution after accounting for the other moderators, as indicated by generally low PIPs and the absence of significant coefficients across model specifications. However, due to pronounced class imbalance across cathode chemistries, low PIP should not be interpreted as evidence of no effect. To assess whether the strong dominance of the NMC baseline category influences this conclusion, we conduct an additional subsampling sensitivity analysis reported in the Supplementary Materials (S.10). Furthermore, since feasible operating voltages are closely tied to cathode chemistry, cut-off charge voltage may absorb some chemistry-related variation in the multivariate setting. Consistent with this interpretation, the cathode-by-voltage interaction specification yields significant interaction terms (Table S6). The persistence of this pattern in the subsampling analysis (Table S5) suggests that, once operational stressors are controlled for, the

variance uniquely attributable to cathode chemistry is smaller than the variance driven by usage conditions. A similar pattern is observed for different cell formats, where neither pouch, prismatic, cylindrical, nor coin cells demonstrate consistent explanatory power. For anode materials, silicon-based technologies exhibit a PIP slightly above 0.65, suggesting moderate relevance. While the coefficient becomes statistically significant at the 10 % level in the PIP $\geq$ 0.65 model, it remains non-significant in the full and PIP $\geq$ 0.50 specifications. This implies that evidence for higher DegRate in silicon-based anodes, relative to the graphite baseline, is weak and model dependent. The result should be interpreted with caution, particularly because it is supported by only one of the models and does not reach a strong level of statistical significance. Nonetheless, it aligns with known degradation mechanisms in silicon, such as volume expansion and structural instability during cycling [3,63,64]. Some variables show statistically significant effects in the MRA despite having low PIP in the BMA, suggesting that their importance may be limited to certain model specifications rather than being broadly robust. For instance, the constant voltage (CV) charging protocol (PIP = 0.492) is associated with lower DegRate, indicated by a significant coefficient of -0.258 percentage points, potentially due to reduced stress during the final phase of charging.

Finally, the degradation curve emerges as a highly robust explanatory factor, with a PIP of 1.000, indicating its consistent relevance across all model specifications. Specifically, when the degradation follows a decelerated pattern, the reported DegRate is significantly higher. This relationship is confirmed by the MRA, where the coefficient remains positive and statistically significant across all three model variants. The consistent significance of this variable suggests that the shape of the degradation trajectory should be accounted for when considering the design and development of battery systems. Charge and discharge rates demonstrate neither statistical significance nor high PIPs. This ambiguity is consistent with the descriptive subgroup patterns in Figure 3. In a multivariate meta-regression, identifying the average main effect of C-rate can be difficult when charge or discharge rate is correlated with other experimental choices and when DegRate is governed by regime-dependent combinations of conditions. Accordingly, the apparent rate effects likely reflect an imbalanced coverage of the experimental design space rather than a universal main effect of charge and discharge rate by themselves. We examined whether publication-specific factors affect reported DegRate by including moderators for publication year, Google Scholar citations, an industry-affiliation dummy variable, and a dummy distinguishing conference proceedings from journal articles. These moderators enable us to examine how publication context and temporal developments may relate to reported outcomes. None of these variables surpassed the PIP threshold in the reduced meta-regressions, and none reached statistical significance in the full-sample model, suggesting that they do not systematically explain variation in reported DegRate.

To reinforce the reliability of our findings, both weighting schemes (as explained in Section 2.3) were applied across the same three model specifications used in the unweighted regressions (Table S7).[3] Overall, the core results remained largely stable, confirming the robustness of key findings; however, some effects proved sensitive to the weighting method. The charge cut-off voltage exhibited a consistently strong positive effect across all WLS2 specifications (ALL-WLS2, 0.50-WLS2, 0.65-WLS2), while in WLS1 it was not significant in ALL-WLS1 and 0.50-WLS1, and attained only marginal significance in 0.65-WLS1. The decelerated degradation trajectory retained its significance under every WLS1 setting but not in any of the WLS2 models, while the manufacturer variable remained significant in all WLS2 variants, yet in WLS1 it was only marginally significant in All-WLS1 and not significant in 0.50-WLS1 and 0.65-WLS1. Despite its low PIP, the CV charge protocol demonstrated a consistent negative and significant effect in every WLS1 specification but lost significance across all WLS2 models, suggesting a model- or context-specific influence. Finally, the fluctuating signs of the charge and discharge rate coefficients further support their lack of robust explanatory power. Overall, the pattern and interpretation of the main results remain unchanged across the unweighted and weighted specifications, with temperature remaining a robust driver while some secondary effects are more sensitive to the weighting choice. In other words, even when using alternative weighting schemes, the robust analysis underscores the stability of the main drivers identified, while also highlighting the sensitivity of some effects to model specifications. This reinforces the importance of methodological transparency in experimental battery research.

Additional sensitivity analyses were performed to evaluate the impact of using linear extrapolation to estimate DegRate from partial cycling data for cells that did not reach 80% of their initial capacity. Approximately 55% (344 out of 627) of DegRates in the regression dataset are estimated using partial cycling data because the 80% end-of-life threshold was not reached. In these cases, DegRate is calculated by dividing the observed capacity fade by the number of cycles up to the last reported cycle, similar to Dechent et al. [9]. This assumes a linear extrapolation of the DegRate beyond the observed window. To show that this approach does not affect our primary results, we calculate DegRate at the 90% threshold for all accelerated and decelerated degradation trajectories crossing the 80% threshold. For each case, we calculate the ratio of the 90% DegRate to the 80% DegRate for each curve shape. For accelerated and decelerated degradation trajectories, we take the median of this ratio (Figure S6) and use it to adjust DegRates for observations that do not reach 80%, while leaving DegRates for observations that reach 80% unchanged. This yields two new effect sizes: DegRate for the decelerated curve and DegRate for the accelerated curve. We then use these new effect sizes to recalculate the BMA and confirm the robustness of the results. The corresponding sensitivity BMA results are reported in Table S9. Since the adjustment applies the trajectory-specific median ratio to all observations that do not reach the 80% EoL threshold, these sensitivity specifications are conservative

[3] *The first (WLS1) regression weights each study by the inverse of its sample size, while the second (WLS2) applies a custom study-quality weight that discounts papers with missing reported information.*

worst-case scenarios that illustrate the potential impact of linear extrapolation on DegRate-based benchmarking. A comparison of Table S9 with the main BMA results shows that the key findings remain substantively unchanged, indicating that our conclusions are robust with respect to the linear extrapolation procedure. All subsequent analyses are based on the reduced dataset used for the regression and BMA, which includes 88 studies and 627 observations.

3.3 Temporal Trends in Battery Degradation Research

The simultaneous analysis of moderators influencing reported DegRate reveals that a range of experimental and methodological characteristics consistently shape degradation outcomes. However, it remains unclear whether technological advances or shifts in research focus have altered degradation behavior and how key influencing factors have evolved over time.

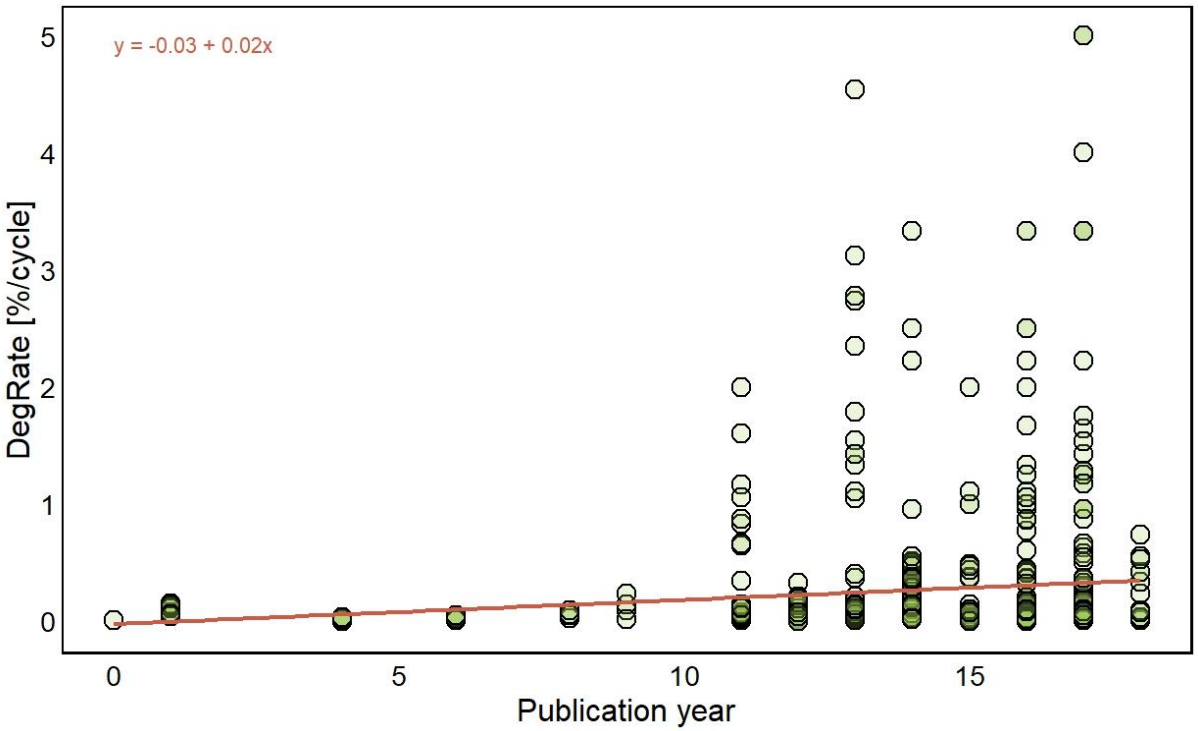

Figure 4: Scatterplot of degradation rate (DegRate) by publication year. The earliest publication in our dataset is from 2006, which represents year 0 in the figure. The standard error of the slope is 0.009, the t-value is 2.331, and the p-value is 0.020. This figure is based on the same dataset of 88 studies and 627 observations as used in the prior meta-regression analyses.

To assess whether DegRate has changed systematically over time, it was analyzed as a function of each study's publication year. The same dataset used in the regression analysis was employed (n = 88, m = 627), with 2006 serving as the reference point (Year 0). Contrary to expectations, technological progress over time has not led to a general reduction in DegRate. As shown in Figure 4, the regression estimate indicates an average increase in DegRate of approximately 0.02 %/cycle per year. A notable rise in variance appears after 2017, suggesting that interest in the topic intensified around this time and that fundamental research began to explore more extreme conditions, contributing to the broader spread of observed DegRate. This increased variability may also reflect greater material innovation, potentially leading to a higher DegRate. At the same time, this trend raises the question of whether publication selection bias is at play – i.e., whether studies reporting more striking values are more

likely to be published. However, few primary studies report standard errors for their effect sizes, which are essential for publication bias tests and standard funnel plot analyses [96–98]. As the first meta-analysis to systematically evaluate battery DegRate across different types of batteries and operating conditions, our study highlights this reporting gap and emphasizes the importance of including such statistical information in future studies. This would enable more robust meta-analytical techniques, including the assessment of potential publication bias. To better understand the observed increase in DegRate over time, we examined how the temperature conditions tested varied by publication year (Figure 5).

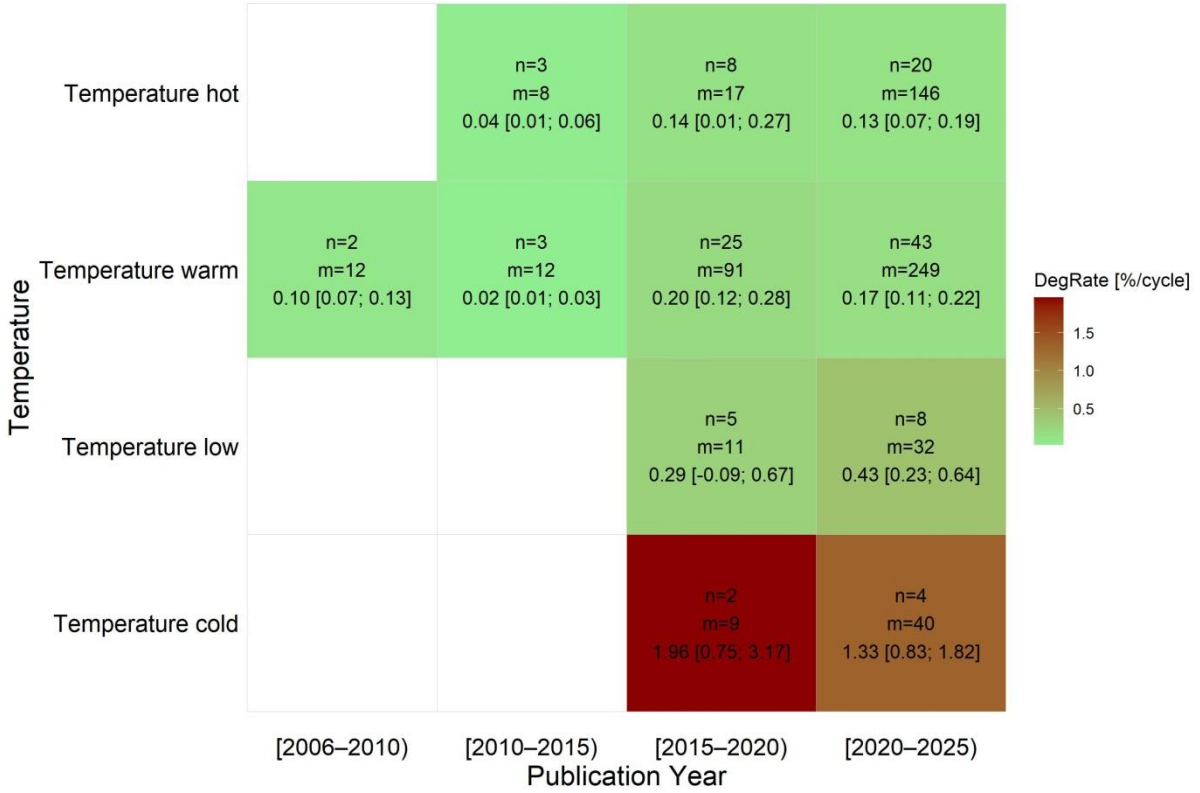

Figure 5: Heatmap of mean DegRate with 95 % confidence intervals, grouped by temperature category and publication year range. Temperature categories are defined as follows: cold <0 °C, low [0–20 °C), warm [20–40 °C), and hot ≥40 °C. The number of observations (m) and number of studies (n) for each combination are shown. Colors range from green (low DegRate) to red (high DegRate), indicating the magnitude of the mean DegRate in each category. This figure is based on the same dataset of 88 studies and 627 observations used in the regression analyses.

The combination of test temperature and publication year reveals a clear shift in research focus over time. Studies published before 2010 were almost exclusively limited to moderate temperature ranges (20–40 °C). It was only after 2010 that high-temperature conditions (≥40 °C) began to be investigated regularly, though without a corresponding rise in DegRate, suggesting that batteries maintain robust performance under elevated temperature conditions. Subzero temperatures (<0 °C) were not systematically included before 2015. More recent studies reporting elevated DegRates under these conditions, likely due to effects such as lithium plating and limited electrode kinetics. Interestingly, the most recent period (≥2020) still shows elevated degradation at subzero temperatures, though slightly improved compared to earlier observations, indicating that newer materials and designs have begun to mitigate some of the severe degradation previously observed. Additionally, the number of studies (and

observations) has increased considerably over time, especially after 2015, reflecting growing research interest and broader experimental coverage. This trend suggests that testing protocols have become progressively more realistic and stress-oriented over time, improving our understanding of battery performance under both moderate and extreme conditions. At the same time, the persistent challenges observed at subzero temperatures highlight the need for continued innovation in materials and designs to ensure reliable operation in harsh environments.

This shift towards more extreme testing conditions over time is not limited to temperature, as summarized in Figure S7. Similar patterns emerge for other experimental parameters, such as cut-off charge voltage, cut-off discharge voltage, and C-rates. However, across all three variables, extreme values predominantly appear in recent years. In line with our heterogeneity analysis, the shift towards higher C-rates does not correspond to a systematic increase in DegRate. Beyond experimental parameters, the temporal heatmaps for anode chemistry, cathode chemistry and cell format demonstrate that recent studies generally report higher DegRate values. To highlight the most notable technologies discussed in the literature, we focus on key subcategories, such as silicon-based anodes and LMO cathodes, independently of the broader groupings used in the meta-regression.

Graphite is the most frequently studied anode material across all years, highlighting its role as the industry baseline. The higher DegRate observed in more recent studies is likely driven by increasingly aggressive testing conditions rather than intrinsic material deterioration. In contrast, Si-based anodes only appear in recent years and already exhibit an elevated DegRate, which is consistent with their well-documented volume expansion and mechanical instability during cycling [3,60,63,64]. Among cathodes, LFP only enters the dataset from 2015 onwards. Apart from LCO, most cathode types exhibit broadly comparable DegRates in recent years. The consistently higher DegRate observed for LCO aligns with its recognized limitations in terms of cycle life [59,60]. In terms of cell format, coin cells only appear after 2015, according to the literature primarily in materials research, where their small size and limited thermal buffering likely contribute to higher DegRate [73,74]. Cylindrical cells demonstrate a clear temporal shift from low (green) to high (red) DegRate, indicating increasingly challenging operating conditions. Prismatic cells consistently demonstrate lower DegRate, presumably due to superior thermal management and mechanical stability, although they are studied less frequently. Pouch cells exhibited comparatively high DegRates between 2015 and 2020, after which it dropped substantially, likely reflecting improvements in sealing, materials or thermal control.

While the heatmaps provide a descriptive overview of temporal shifts in degradation behavior, formal testing is required to determine whether these patterns represent systematic trends. To this end, we extend the meta-regression framework by introducing an interaction term between publication year and temperature. Publication year is already included as a moderator in the full models, but it is explicitly added to the PIP-restricted specifications to ensure that the interaction term can be properly interpreted. All other model settings remain unchanged. The regression analysis revealed a significant negative interaction between publication year and temperature, see Table 3. The positive main effect of

temperature suggests that higher temperatures are associated with higher DegRate in the base year. However, this effect weakens over time. For each additional year, the temperature effect decreases by 0.027 percentage points. This pattern shows that, although earlier technologies were more susceptible to degradation in warm conditions, this disadvantage has decreased over time. The reversal in the sign of the interaction suggests that recent technologies may appear to deteriorate more rapidly in cold environments than in warm ones, reflecting improved heat resistance. Conversely, the positive main effect of publication year (0.597 percentage points) shows that degradation increases over time, but this effect diminishes by 0.027 percentage points for every additional degree Celsius. However, the apparent trend of higher degradation under cold conditions in recent studies is likely due to earlier studies not testing such temperatures. Accordingly, the positive year-on-year effect on DegRate should not be interpreted as technological deterioration, but rather as a consequence of the increased prominence of cold-temperature conditions in more recent studies, in which higher degradation is observed.

Table 3: MRA with interaction term

Moderator variable	ALL-UW	0.50-UW	0.65-UW	ALL-WLS1	0.50-WLS1	0.65-WLS1	ALL-WLS2	0.50-WLS2	0.65-WLS2
INTERCEPT	-2.716*	-3.171**	-3.870**	-2.319	-1.436	-2.190*	-3.740**	-4.073***	-4.882**
	(-1.884)	(2.598)	(-2.584)	(-1.602)	(-1.085)	(-1.957)	(-2.414)	(-2.802)	(-2.363)
PUBLICATION: YEAR	0.597**	0.517*	0.517*	0.584**	0.269	0.365*	0.901**	0.825**	0.820*
	(2.239)	(1.769)	(1.800)	(2.075)	(1.233)	(1.718)	(2.389)	(2.123)	(1.889)
EXPERIMENT: TEMPERATURE	0.059**	0.035	0.032	0.040*	0.010	0.018	0.087**	0.060	0.054
	(2.122)	(1.261)	(1.215)	(1.687)	(0.590)	(1.240)	(2.069)	(1.516)	(1.406)
INTERACTION: TEMP x YEAR	-0.027***	-0.018*	-0.017*	-0.019**	-0.008	-0.011*	-0.037**	-0.028*	-0.026*
	(-2.647)	(-1.710)	(-1.701)	(-2.142)	(-1.267)	(-1.845)	(-2.484)	(-1.884)	(-1.785)
All other Moderators included as controls (Table 2)									
Studies (observations)	88 (627)	88 (627)	88 (627)	88 (627)	88 (627)	88 (627)	88 (627)	88 (627)	88 (627)
R^2 (adjusted)	0.351	0.328	0.323	0.310	0.241	0.221	0.353	0.348	0.342

Notes: The results are reported for unweighted (UW) meta-regression, weighted meta-regression using the inverse number of observations per study as weights (WLS1), and weighted meta-regression using the study-quality index as weights (WLS2). For each approach, three specifications are shown: the full model including all moderators (ALL), a restricted model including only moderators with posterior inclusion probability (PIP) ≥ 0.50, and a more stringent restricted model including only moderators with PIP ≥ 0.65. All models include an interaction term between publication year and temperature. In the PIP-restricted models, publication year is additionally included as a moderator to allow interpretation of the interaction. The t-statistics are reported in parentheses. The significance level for 0.1, 0.05, 0.01 corresponds to "", "**" and "***" respectively. The base categories for the dummy variables were chosen as the most frequently observed specifications: [1]NMC, [2]graphite, [3]cylindrical cell, and [4]linear degradation trajectory. Only the results of the interaction between year and temperature are reported because the results of the meta-regression for the other moderators are consistent with those of the meta-regression without interaction across all model specifications.*

The other model specifications confirm that the effect of temperature on DegRate is time-dependent, with higher degradation observed in recent studies driven by cold conditions. Although the interaction model implies a time-dependent temperature effect, publication year is not a significant moderator in the MRA without the interaction term. Therefore, the apparent time trend is not driven by the year itself, but rather by the more frequent use of cold-temperature testing in recent studies. When additional moderators are included, the year effect disappears, suggesting that cold conditions account for only some of the underlying variation. The MRA results for all other moderators were consistent with those obtained in the models without the interaction term, highlighting the reliability of the findings.

3.4 Pairwise Relationships Among Degradation Factors

While the meta-regression framework allows us to identify the primary drivers of degradation by

jointly estimating their effects, it does not reveal which combinations of conditions were tested or their relationship to the observed outcomes. To address this issue, we supplement the regression analysis with a pairwise examination of moderator combinations. For this purpose, temperature and cut-off charge voltage, both of which are significant and robust moderators in the meta-regression, were chosen as fixed reference variables. DegRate was then analyzed in combination with other moderators. This approach highlights gaps in literature and illustrates which factor interactions are associated with particularly high DegRate.

The results confirm our hypothesis that extreme combinations of moderators are rarely investigated. Figure 6 illustrates this for the cut-off charge voltage, which was identified as a significant moderator in the MRA heterogeneity analysis. While moderate cut-off voltages in the range of 3.0 to 4.0 V are associated with a relatively low DegRate across all temperatures, the combination of higher cut-off voltages (>4.0 V) and sub-zero temperatures results in degradation increasing by over 1 %/cycle. These stress conditions exacerbate known mechanisms such as lithium plating and accelerated SEI degradation, which are particularly severe when cold temperatures coincide with high charging voltages. White grid fields indicate combinations with no experimental data, marking unexplored regions, whereas cells supported by only few studies or observations represent weakly explored conditions. Together, these gaps highlight opportunities for future research.

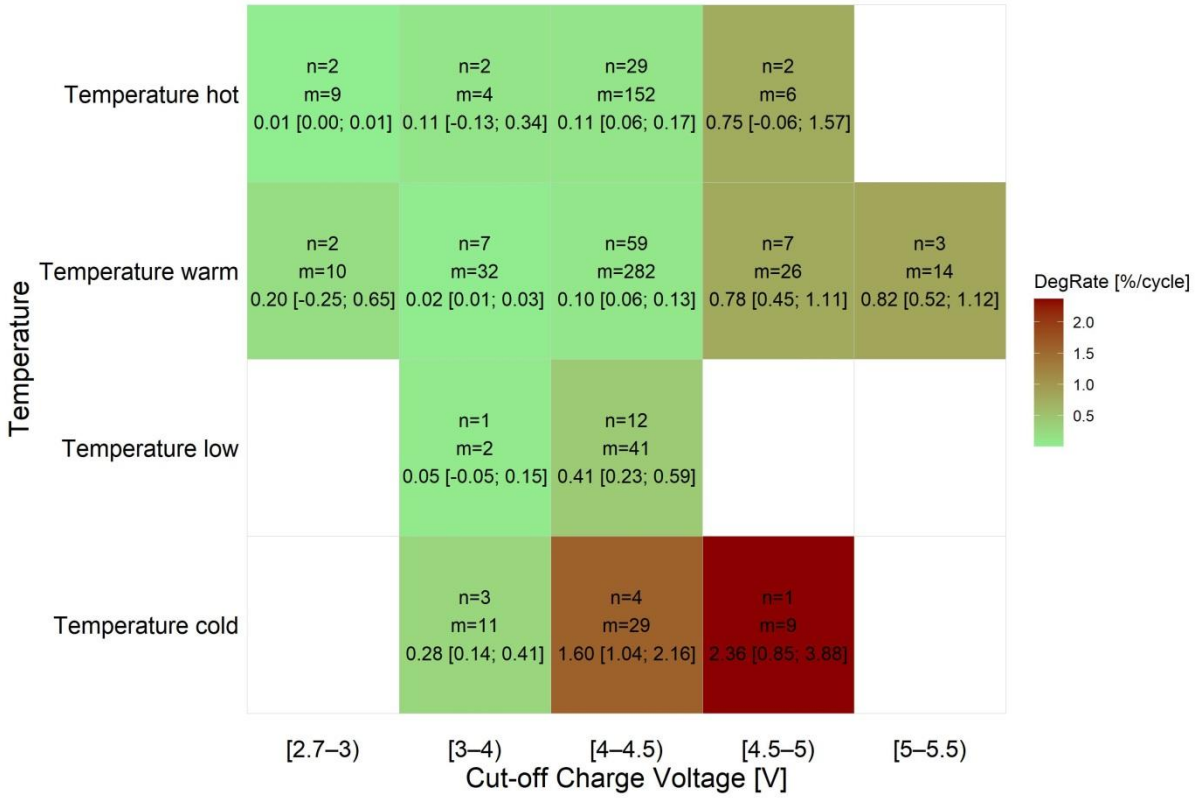

Figure 6: Heatmap of mean DegRate with 95 % confidence intervals, grouped by temperature category and cut-off charge voltage. Temperature categories are defined as follows: cold <0 °C, low [0–20 °C), warm [20–40 °C), and hot ≥40 °C. The number of observations (m) and number of studies (n) for each combination are shown. Colors range from green (low DegRate) to red (high DegRate), indicating the magnitude of the mean DegRate in each category. This figure is based on the same dataset of 88 studies and 627 observations used in the regression analyses.

The analysis of the combined effects of cathode and anode chemistry on temperature reveals additional differences (Figure 7). The distribution of studies and observations across cathode chemistries highlights a pronounced class imbalance, which limits inference for minority chemistries and provides context for the low PIPs observed in the multivariate analysis. LFP and LMO-based cathodes show consistently low mean DegRate across all available temperature ranges, supported by a relatively large number of observations, particularly in the warm (20–40 °C) and hot (≥40 °C) conditions. These findings reinforce the well-documented thermal and electrochemical stability of these cathode chemistries. However, no studies were identified for LMO-based cathodes under cold conditions (<0 °C), indicating a gap in experimental research for this material class in low-temperature environments. By contrast, NMC cathodes exhibit a sharp increase in DegRate under cold conditions (<0 °C) exceeding 2 %/cycle based on 25 observations from 3 studies. This is consistent with their known tendency for structural transitions toward spinel and rock-salt phases during delithiation, which are accompanied by oxygen release and contribute to degradation. NCA cathodes display a similar vulnerability, with values around 1.3 %/cycle, though this is based on only two observations from one study. Overall, studies have shown that nickel-rich NMC and NCA cathodes are susceptible to structural instability under cold conditions [99–101]. However, Wittmann [102] observed only weak temperature dependence for NCA, whereas NMC cathodes exhibited pronounced degradation as the ambient temperature decreased. While visually striking, these results must be interpreted with caution due to the limited evidence base. Meanwhile, LCO cathodes show slightly elevated mean DegRate even under warmer conditions. Among anode materials, graphite is the most frequently studied across all temperature categories, with particularly high data density in the warm (20–40 °C) and hot (≥40 °C) conditions (n = 289 and n = 144, respectively), lending strong statistical weight to the observed low DegRate. Overall, DegRate remain comparatively low for graphite-based cells across all temperature ranges, reinforcing their stability. LTO, MCMB, and other carbon-based anodes are less frequently represented, limiting the interpretability of their patterns, especially under low and cold conditions where data are sparse or missing. Notably, silicon-containing anodes exhibit a high mean DegRate exceeding 2 %/cycle under cold conditions (<0 °C). This is consistent with the volumetric expansion that occurs during the lithiation of silicon-based anodes, which is associated with lithium and capacity loss. Although this is a striking result, it is based on just two observations from one study and should therefore be treated with caution due to limited statistical reliability. Nevertheless, this result highlights the well-documented mechanical and interfacial instability of these technologies, which are still under development. These chemistry-dependent temperature responses highlight the relevance of electrode materials for degradation behavior, motivating our subsequent model-implied benchmarks for graphite/Si-based anodes and LFP/NMC cathodes, which are the most widespread chemistries.

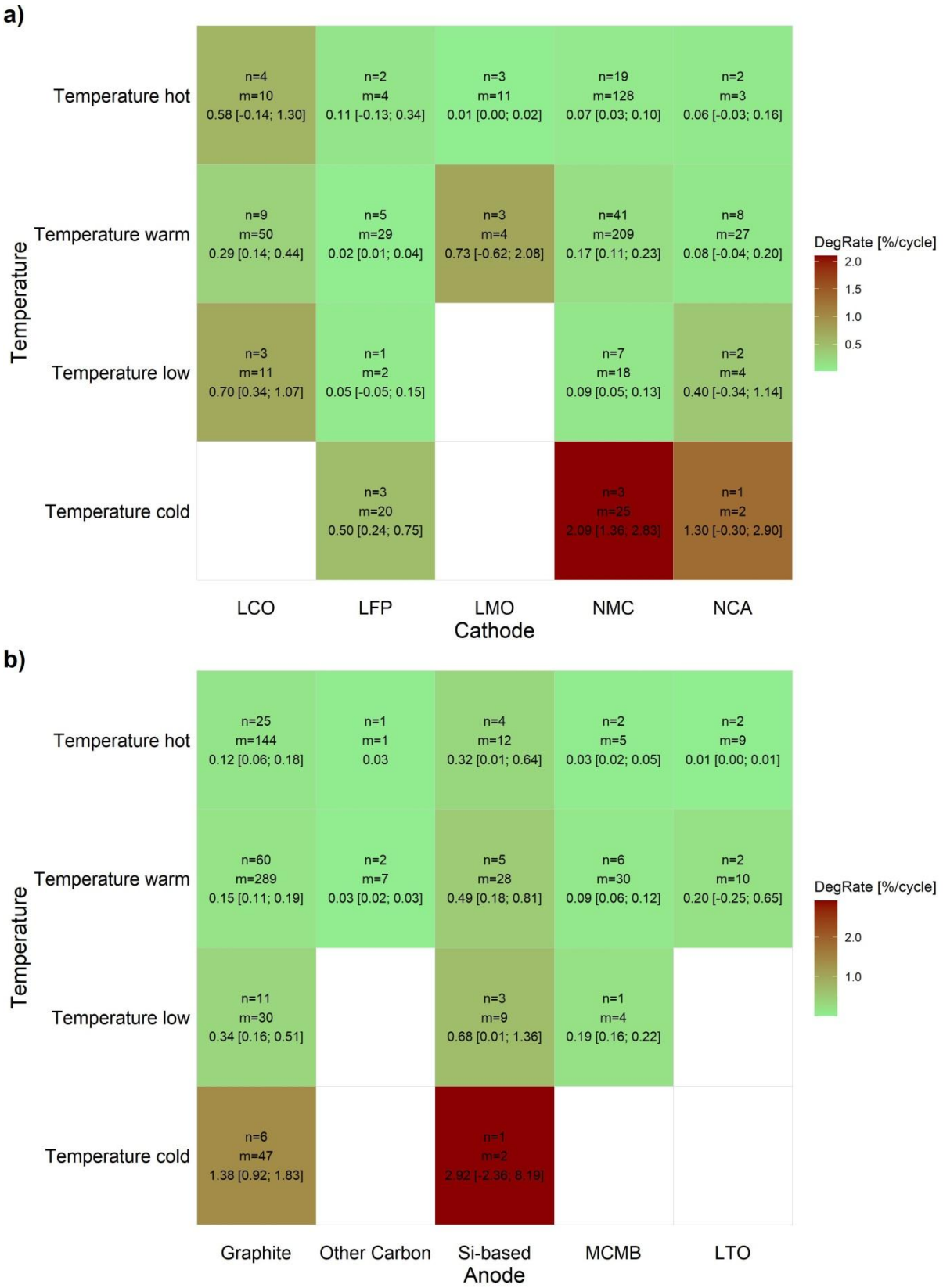

Figure 7: Heatmap of mean DegRate with 95 % confidence intervals, grouped by temperature category against a) cathode and b) anode. Temperature categories are defined as follows: cold <0 °C, low [0–20 °C), warm [20–40 °C), and hot ≥40 °C. The number of observations (m) and number of studies (n) for each combination are shown. Colors range from green (low DegRate) to red (high DegRate), indicating the magnitude of the mean DegRate in each category. This figure is based on the same dataset of 88 studies and 627 observations used in the regression analyses.

For additional moderators, complementary analyses with temperature, including cut-off discharge voltage, cell format, and C-rate, are summarized in Figure S8. In contrast to the cut-off charge voltage

results, the cut-off discharge-voltage analysis reveals an unexpected pattern, with lower cut-off voltages not appearing to be more harmful than higher ones, although such conditions are discussed in the literature in connection with SEI-related side reactions. These findings should nevertheless be interpreted with caution, given the limited number of studies and observations in several cells of the matrix. However, combinations involving extremely low cut-off voltages and cold temperatures have not been tested, leaving this critical scenario largely unexplored. The analysis of the combined effects of cell format and temperature reveals distinct differences in degradation susceptibility. Only cylindrical and pouch cells have undergone testing across the full temperature range. Both formats exhibit pronounced degradation under cold conditions, though pouch cells perform slightly better. For instance, in the low-temperature range, the mean DegRate is 0.20 [−0.04; 0.44] %/cycle for pouch cells, compared to 0.52 [0.28; 0.77] %/cycle for cylindrical cells. At elevated temperatures, rectangular formats (pouch and prismatic) demonstrate a consistently lower DegRate than coin and cylindrical cells. This may be due to more application-relevant test conditions, as well as superior thermal management that promotes uniform heat dissipation. In contrast, the spiral-wound architecture of cylindrical cells can generate uneven internal temperature distributions, resulting in thermal imbalances that induce mechanical stress and accelerated degradation. The pattern observed for coin cells reflects their primary use in materials research. Their compact design and limited thermal mass make them particularly susceptible to thermal stress. The analysis of the combined effects of temperature and C-rate indicates that high charge rates at low temperatures are particularly critical for degradation. While at moderate to high temperatures (≥20 °C), the DegRate remains relatively stable regardless of charging or discharging speed, the combination of subzero conditions with fast charging or discharging leads to a substantially elevated DegRate. This highlights that electrochemical processes under cold conditions are especially sensitive to current load. Under such conditions, lithium plating and structural disordering may occur. Notably, the literature contains very few studies examining extremely high charge or discharge rates at subzero temperatures, likely due to technical limitations or safety concerns during experimental design. These patterns also clarify why the effects of C-rates appeared ambiguous in the meta-regression. As the full spectrum of C-rates has only been systematically tested at elevated temperatures, where degradation tends to remain low, the apparent tendency of higher C-rates to reduce DegRate in the MRA results likely reflects this testing bias rather than a true, general effect. Finally, Figure S9 presents heatmaps corresponding to the cut-off charge voltage on the y-axis. These reveal the same pattern and support the temperature-based pairwise relationships presented above.

3.5 Model-implied Benchmark Inference for Future Experimental Research

This meta-analysis demonstrated that DegRate is shaped by a wide range of experimental and methodological moderators. To explore their combined implications, we created a hypothetical study design using the coefficients from the unweighted PIP ≥ 0.50 model (Table 2, 0.50-UW model).

Unlike the descriptive heatmap analysis, which is limited to pairwise comparisons, this model-implied inference framework incorporates all significant moderators simultaneously. It hereby allows us to estimate DegRates conditional on the existing evidence base for any combination of input parameters, providing reference values for scenarios that have already been tested (in-sample) and prospective benchmarks for those that have not (out-of-sample), against which future studies can be evaluated. It is important to emphasize that these estimates do not represent experimentally validated predictions. Instead, they constitute model-implied inferences derived from the available literature and are intended to serve as hypothesis-generating benchmarks for future experimental validation. These simulated benchmarks represent the current state of the art as implied by the meta-analytic evidence and define targets that future experimental work should strive to exceed. The analysis focuses on NMC and LFP cathodes, as well as graphite and Si-based anodes, which are the most frequently represented electrode materials in the meta-dataset, reflecting their central relevance in current lithium-ion battery research. To align with practical operating ranges, we limited the benchmark estimates to upper cut-off voltages of 3.0–4.4 V for LFP cells and 3.6–5.0 V for NMC cells, extending their typical voltage limits (≈ 3.65 V for LFP and 4.2 V for NMC). The cut-off discharge voltages were set to 2.5 V and 3.0 V for LFP and NMC, respectively [59,103]. To approximate a best practice benchmark, we set the dummy variables to conceptually neutral values. Specifically, we assumed that the batteries were free of defects to ensure that the estimated DegRates represent the normal operating state, enabling us to focus on assessing the experimental moderators. Similarly, we avoided confounding with market- or manufacturer-specific effects by keeping the manufacturer unknown. This emphasizes the technological drivers of degradation and reflects the non-commercial focus of much experimental research. Finally, the degradation path was fixed to the decelerated curve described in the literature as a favorable trajectory associated with long service lifetimes [39]. Figure 8 shows the temperature and cut-off charge voltage benchmark estimates, which were identified as significant experimental moderators in the meta-regression analysis. Temperature is divided into four categories (cold, low, warm and hot), which are consistent with those already used in the heatmap analysis. The x-axis represents the cut-off charge voltage, and the y-axis shows the estimated DegRate. The four electrode chemistries (LFP+Graphite, LFP+Si-based, NMC+Graphite and NMC+Si-based) are shown as separate trajectories. The model provides in-sample benchmark estimates for combinations of voltage, temperature, and electrode chemistry that appear in the meta-dataset, visualized as solid line segments and filled markers. Combinations not examined in any primary study result in out-of-sample extrapolation and are shown as dotted line segments and unfilled markers. For the estimation grid, the cut-off charge voltage was sampled in uniform 0.2 V increments. A sampled voltage point is considered in-sample when at least one primary study reported experimental data within the corresponding voltage region. Otherwise, it is treated as out-of-sample. In contrast to in-sample estimates, out-of-sample estimates rely on extrapolation beyond the locally observed operating combinations and therefore primarily serve to identify regions of the experimental design space where empirical evidence is currently sparse and targeted experimental validation would be particularly

informative for testing these extrapolated benchmarks. Thus, they should be interpreted as prospective, model-implied benchmarks for currently unexplored stress regimes, rather than validated performance expectations. Consistent with this interpretation, these estimates are associated with increased uncertainty, which is transparently reflected in typically wider confidence intervals. Full results, including 95 % confidence intervals, are provided in Table S10.

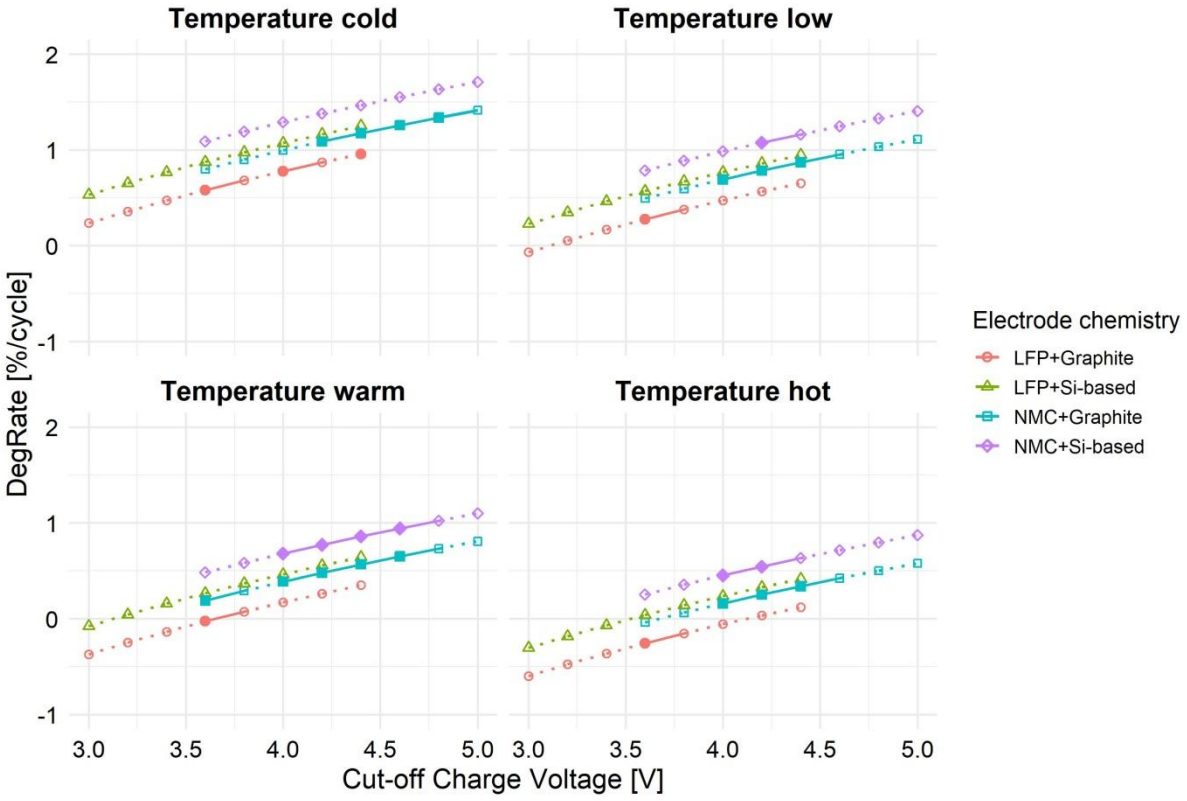

Figure 8: The figure shows the model-implied benchmark estimates of DegRate based on the unweighted meta-regression model, with posterior inclusion probability restricted to >50 % (Table 2, 0.50-UW model). These results vary according to the cut-off charge voltage on the x-axis and the four temperature categories (cold: <0 °C; low: [0, 20); warm: [20, 40); hot: ≥40 °C) across the four electrode chemistries (LFP+Graphite; LFP+Si-based; NMC+Graphite; NMC+Si-based). Solid line segments and filled markers indicate combinations of voltage, temperature, and chemistry that are present in the underlying dataset, whereas dotted line segments and unfilled markers represent out-of-sample extrapolations for combinations not observed in the original sample. For the estimation grid, the cut-off charge voltage was sampled in uniform 0.2 V increments. A sampled voltage point is considered in-sample when at least one primary study reported experimental data within the corresponding voltage region. Otherwise, it is treated as out-of-sample. The trajectories represent the fitted mean values, and Table S10 provides 95 % confidence intervals (CI).

The performance ranking at high cut-off voltages remains consistent across all temperature categories: LFP+Graphite ≻ NMC+Graphite ≈ LFP+Si-based ≻ NMC+Si-based. Therefore, graphite-containing batteries represent the established baseline, whereas silicon-based systems, particularly in combination with LFP, are promising but more vulnerable alternatives. Importantly, the most extreme operating points shown in Figure 8 are the least well-covered by the available literature. Therefore, they are associated with increased uncertainty, as quantified by the reported confidence intervals (Table S10). Under extreme test conditions (below 0 °C and a cut-off voltage of 4.4 V), LFP+Si-based cells have an average DegRate of 1.25 %/cycle. This corresponds to 16 cycles before reaching the 80 % capacity threshold. NMC+Si-based cells perform even worse at extreme voltage condition of 5.0 V, with an average DegRate of 1.71 %/cycle and an implied lifetime of around 11 cycles. By contrast, graphite-

based chemistries demonstrate lower DegRate under the same conditions, with NMC+Graphite degrading at an average rate of 1.41 %/cycle (approximately 14 cycles), while LFP+Graphite degrades at a rate of 0.96 %/cycle (approximately 20 cycles). These quantitative benchmarks should be interpreted alongside the confidence intervals presented in Table S10, which highlight the uncertainty arising from uneven coverage across the temperature-voltage range. The effect of voltage limiting is particularly evident when reduced to 3.6 V for LFP and 4.2 V for NMC because these are the maximum cut-off values commonly used in practice. For LFP+Graphite, the average DegRate decreases to 0.58 %/cycle, about 40 % reduction, extending cycle life to around 34 cycles. For LFP+Si-based cells, the corresponding benchmark estimate is 0.87 %/cycle (approximately 22 cycles). Compared with the same chemistry at 4.4 V (approximately 16 cycles), the DegRate is reduced by around 30 %. Reducing the cut-off voltage decreases the DegRate by 23 % for NMC+Graphite (from 1.41 %/cycle to 1.09 %/cycle) and by 19 % for NMC+Si-based (from 1.71 %/cycle to 1.38 %/cycle). Overall, these results suggest that, although Si-based anodes have higher absolute DegRates at both voltage levels, graphite-based systems demonstrate a more pronounced acceleration of degradation when the upper voltage limit is increased. When comparing temperature categories, the DegRate decreases as the temperature increases. For LFP+Si-based technologies, the average DegRate at a temperature of 20–40 °C (warm) and a cut-off voltage of 4.4 V is 0.64 %/cycle, corresponding to lifetime of 31 cycles. This reflects a reduction of around 50 % compared to operations below 0 °C at the same voltage. The temperature effect is even more pronounced for LFP cells with graphite anodes. At identical high-voltage conditions, operating at warm temperature improves the DegRate by approximately 63 % compared to operating at cold temperatures. For NMC+Graphite cells, operating at 5.0 V under warm conditions reduces the DegRate by approximately 42 % compared to operating at cold conditions. For NMC+Si-based cells, the reduction is smaller at around 35 %. Si-based anodes exhibit smaller improvements because the degradation factors discussed in Section 3.1 are likely active regardless of temperature. At higher temperatures, the model yields slightly negative benchmark estimates in the lower voltage range. These values reflect estimation uncertainty rather than true performance improvements and are related to the linear specification of the regression. Overall, the temperature effect is consistent with the results reported by Gao [79]. Although the authors modelled cycle life as a function of C-rate and temperature rather than cut-off voltage, the pattern is similar. They observed no more than 30 cycles at strongly negative temperatures and predicted that lifetimes would be extended at higher temperatures, corresponding to lower DegRate. To examine how the voltage effect depends on cathode chemistry, we present an expanded specification with interaction terms in Table S6. In line with the model-implied benchmark framework, our focus is on the unweighted PIP $\geq$ 0.50 restricted model (0.50-UW). The weighted specifications (0.50-WLS1 and 0.50-WLS2) are included as robustness checks. The results suggest that NMC cells are more sensitive to increases in cut-off voltage than LFP cells, consistent with the literature [104,105].

4 Conclusion

Despite the numerous reviews and primary experimental studies on LIB degradation, a systematic, quantitative assessment of DegRate and its underlying causes has been lacking. We present the first meta-analysis of LIB degradation. Our dataset comprises 146 studies and 917 effect sizes. 46 moderators were identified and categorized into four groups: battery differences, experimental characteristics, measurement characteristics, and publication characteristics. The dataset yielded a mean effect size of 0.23 %/cycle and a median of 0.04 %/cycle, revealing a distribution shifted toward higher DegRates. Building on subgroup and mean effect size analyses, we applied Bayesian model averaging and meta-regression techniques.

The meta-analysis shows that DegRates are more strongly driven by upper cut-off voltage and temperature than by battery-specific factors. Additionally, the analysis reveals significant opportunities for future research within the experimental matrix. Here we found the potential operating LIBs at very high voltage levels of up to 5 V as future perspective and outlook for optimized electrolytes and electrodes and added this to our study. At the same time, we can already provide a model-implied benchmark that accounts for the identified moderators. These benchmarks should be interpreted alongside their 95% confidence intervals (Table S10), which quantify uncertainty arising from uneven evidence coverage across the moderator space. In particular, the most extreme combinations of very low temperature and very high cut-off voltage are currently sparsely covered, such that the corresponding benchmarks are less directly supported by primary studies in this operating region (i.e. rely more strongly on extrapolation) and should be prioritized for targeted experimental validation in future work.

Our results suggest that under extremely cold conditions (<0 °C) and very high cut-off voltages (LFP: 3.8–4.4 V; NMC: 4.4–5.0 V), promising anode-cathode combinations, such as LFP+Si-based [106,107] and NMC+Si-based [108–110] systems, exhibit average model-implied benchmark DegRates of 0.98 %/cycle to 1.25 %/cycle (approximately 16–20 cycles until 20 % capacity fade) and 1.47 %/cycle to 1.71 %/cycle (approximately 11–13 cycles until 20 % capacity fade), respectively. Given uneven evidence coverage in this extreme operating region, these values should be interpreted as prospective benchmarks and read alongside their confidence intervals. For comparison, established chemistries, such as LFP+Graphite and NMC+Graphite, which are more frequently represented in the meta-dataset, show model-implied benchmark DegRates of 0.68 %/cycle to 0.96 %/cycle (20–29 cycles to 20 % capacity fade) and 1.17 %/cycle to 1.41 %/cycle (14–17 cycles to 20 % capacity fade), respectively, under the same extreme conditions. Across chemistries, benchmark precision is higher in well-covered, in-sample regions and lower where evidence is sparse or estimates rely on extrapolation, as reflected in the reported confidence intervals.

Our analysis faces several limitations. First, we had to exclude certain moderators, such as depth of discharge**,** electrolyte composition, and high-power/high-energy labeling, because they were not consistently reported across primary studies. Second, the varying levels of detail with which primary

studies reported experimental information required us to aggregate some moderators into broader categories, which inevitably led to a loss of information. Consequently, it was not possible to account for specific degradation mechanisms. Although the overall dataset is substantial, the coverage of evidence is uneven for some moderators. Accordingly, the results and benchmark estimates are more precise in well-covered regions and are associated with wider uncertainty intervals where evidence is sparse. Third, DegRate is an interval-averaged endpoint metric, summarizing capacity fade up to a common end-of-life threshold rather than fade evolution across the cycling life. Accordingly, combining studies with different trajectory shapes into a single endpoint-based effect size may obscure features of degradation within the cycling life and should therefore be interpreted as a benchmark measure rather than a diagnostic of trajectory shape. In addition, for observations that do not reach the 80% EoL threshold within the reported cycling window, DegRate must be estimated from partial cycling data, which implies a linear extrapolation and may lead to over- or underestimation of degradation. Fourth, since this is a foundational meta-analysis in the field, we could not apply established tests for publication bias or other analyses relying on reported standard errors, since most primary studies do not report them**.** However, our meta-analysis contributes to the accumulation of knowledge on LIB degradation and provides a framework for explaining the heterogeneity of degradation outcomes.

The potential for future research is demonstrated, and a benchmark for upcoming studies is offered, particularly with respect to moderator combinations that have not yet been experimentally tested. Research in the future should aim to exceed these benchmarks. Insights from this meta-analysis highlight the importance of in-depth investigations to improve the cycling performance of LIBs. As the evidence base continues to grow, future studies may update and extend this synthesis using the same search strategy and analytical framework.

5 Reference

[1] R. Li, N.D. Kirkaldy, F.F. Oehler, M. Marinescu, G.J. Offer, S.E.J. O'Kane, The importance of degradation mode analysis in parameterising lifetime prediction models of lithium-ion battery degradation, Nat. Commun. 16 (2025) 2776. https://doi.org/10.1038/s41467-025-57968-3.

[2] T. Rahman, T. Alharbi, Exploring Lithium-Ion Battery Degradation: A Concise Review of Critical Factors, Impacts, Data-Driven Degradation Estimation Techniques, and Sustainable Directions for Energy Storage Systems, Batteries 10 (2024) 220. https://doi.org/10.3390/batteries10070220.

[3] D.H. Jeon, S. Kim, R. Hempelmann, State-of-the-art review of degradation mechanisms of commercial lithium-ion batteries, Journal of Power Sources 646 (2025) 237242. https://doi.org/10.1016/j.jpowsour.2025.237242.

[4] X. Han, L. Lu, Y. Zheng, X. Feng, Z. Li, J. Li, M. Ouyang, A review on the key issues of the lithium ion battery degradation among the whole life cycle, eTransportation 1 (2019) 100005. https://doi.org/10.1016/j.etran.2019.100005.

[5] Y. Che, X. Hu, X. Lin, J. Guo, R. Teodorescu, Health prognostics for lithium-ion batteries: mechanisms, methods, and prospects, Energy Environ. Sci. 16 (2023) 338–371. https://doi.org/10.1039/D2EE03019E.

[6] J.S. Edge, S. O'Kane, R. Prosser, N.D. Kirkaldy, A.N. Patel, A. Hales, A. Ghosh, W. Ai, J. Chen, J. Yang, S. Li, M.-C. Pang, L. Bravo Diaz, A. Tomaszewska, M.W. Marzook, K.N. Radhakrishnan, H. Wang, Y. Patel, B. Wu, G.J. Offer, Lithium ion battery degradation: what you need to know, Physical Chemistry Chemical Physics 23 (2021) 8200–8221. https://doi.org/10.1039/D1CP00359C.

[7] S. Ma, M. Jiang, P. Tao, C. Song, J. Wu, J. Wang, T. Deng, W. Shang, Temperature effect and thermal impact in lithium-ion batteries: A review, Progress in Natural Science: Materials International 28 (2018) 653–666. https://doi.org/10.1016/j.pnsc.2018.11.002.

[8] J.S. Menye, M.-B. Camara, B. Dakyo, Lithium Battery Degradation and Failure Mechanisms: A State-of-the-Art Review, Energies 18 (2025) 342. https://doi.org/10.3390/en18020342.

[9] P. Dechent, A. Epp, D. Jöst, Y. Preger, P.M. Attia, W. Li, D.U. Sauer, ENPOLITE: Comparing Lithium-Ion Cells across Energy, Power, Lifetime, and Temperature, ACS Energy Letters 6 (2021) 2351–2355. https://doi.org/10.1021/acsenergylett.1c00743.

[10] A.B. Haidich, Meta-analysis in medical research, Hippokratia 14 (2010) 29–37.

[11] E. Hariton, J.J. Locascio, Randomised controlled trials - the gold standard for effectiveness research: Study design: randomised controlled trials, BJOG 125 (2018) 1716. https://doi.org/10.1111/1471-0528.15199.

[12] M. Robin DiMatteo, P.J. Giordani, H.S. Lepper, T.W. Croghan, Patient Adherence and Medical Treatment Outcomes: A Meta-Analysis, Medical Care 40 (2002) 794. https://doi.org/10.1097/00005650-200209000-00009.

[13] P.F. Whiting, R.F. Wolff, S. Deshpande, M. Di Nisio, S. Duffy, A.V. Hernandez, J.C. Keurentjes, S. Lang, K. Misso, S. Ryder, S. Schmidlkofer, M. Westwood, J. Kleijnen, Cannabinoids for Medical Use: A Systematic Review and Meta-analysis, JAMA 313 (2015) 2456–2473. https://doi.org/10.1001/jama.2015.6358&utm_campaign=articlePDF%26utm_medium=articlePDFlink%26utm_source=articlePDF%26utm_content=jama.2015.6358.

[14] J. Geyer-Klingeberg, M. Hang, A.W. Rathgeber, What drives financial hedging? A meta-regression analysis of corporate hedging determinants, International Review of Financial Analysis 61 (2019) 203–221. https://doi.org/10.1016/j.irfa.2018.11.006.

[15] M. Hang, J. Geyer-Klingeberg, A. Rathgeber, S. Stöckl, Economic Development Matters: A Meta-Regression Analysis on the Relation between Environmental Management and Financial Performance, Journal of Industrial Ecology 22 (2018) 720–744. https://doi.org/10.1111/jiec.12573.

[16] T.D. Stanley, S.B. Jarrell, Gender Wage Discrimination Bias? A Meta-Regression Analysis, The Journal of Human Resources 33 (1998) 947. https://doi.org/10.2307/146404.

[17] P. Valickova, T. Havranek, R. Horvath, Financial Development and Economic Growth: A Meta-Analysis, Journal of Economic Surveys 29 (2015) 506–526. https://doi.org/10.1111/joes.12068.

[18] T.D. Stanley, C. Doucouliagos, Meta-regression analysis in economics and business, Routledge, London, New York, 2012.

[19] M. Straub-Mück, J. Geyer-Klingeberg, A.W. Rathgeber, Determinants of the long-term degradation rate of photovoltaic modules: A meta-analysis, Renewable and Sustainable Energy Reviews 216 (2025) 115697. https://doi.org/10.1016/j.rser.2025.115697.

[20] J.S. Bulmer, A. Kaniyoor, J.A. Elliott, A Meta-Analysis of Conductive and Strong Carbon Nanotube Materials, Advanced materials 33 (2021) e2008432. https://doi.org/10.1002/adma.202008432.

[21] A. El-Naggar, Z. Chen, W. Jiang, Y. Cai, S.X. Chang, Biochar effectively remediates Cd contamination in acidic or coarse- and medium-textured soils: A global meta-analysis, Chemical Engineering Journal 442 (2022) 136225. https://doi.org/10.1016/j.cej.2022.136225.

[22] Z. Gao, T. Cui, H. Qian, D.J. Sapsford, P.J. Cleall, M.J. Harbottle, Can wood waste be a feedstock for anaerobic digestion? A machine learning assisted meta-analysis, Chemical Engineering Journal 487 (2024) 150496. https://doi.org/10.1016/j.cej.2024.150496.

[23] Z. Gao, H. Qian, T. Cui, Z. Ren, X. Wang, Comprehensive meta-analysis reveals the impact of non-biodegradable plastic pollution on methane production in anaerobic digestion, Chemical Engineering Journal 484 (2024) 149703. https://doi.org/10.1016/j.cej.2024.149703.

[24] M. Imran-Shaukat, R. Apaiyakul, H. Haghani, M. Xiao, H. Gao, Z. Liang, P. Tontiwachwuthikul, T. Sema, The statistical panorama of post-combustion carbon capture via non-aqueous absorbents: A comprehensive meta-analysis, Chemical Engineering Journal 522 (2025) 167010. https://doi.org/10.1016/j.cej.2025.167010.

[25] Y.J. Kim, J. Hyun, A. Michelsen, E.E. Kwon, J.Y. Jung, Key determinants of soil labile nitrogen changes under climate change in the Arctic: A meta-analysis of the responses of soil labile nitrogen pools to experimental warming and snow addition, Chemical Engineering Journal 494 (2024) 153066. https://doi.org/10.1016/j.cej.2024.153066.

[26] P. Maziarka, A. Anca-Couce, W. Prins, F. Ronsse, A meta-analysis of thermo-physical and chemical aspects in CFD modelling of pyrolysis of a single wood particle in the thermally thick regime, Chemical Engineering Journal 446 (2022) 137088. https://doi.org/10.1016/j.cej.2022.137088.

[27] M. Yeganeh, E. Charkhloo, H.R. Sobhi, A. Esrafili, M. Gholami, Photocatalytic processes associated with degradation of pesticides in aqueous solutions: Systematic review and meta-analysis, Chemical Engineering Journal 428 (2022) 130081. https://doi.org/10.1016/j.cej.2021.130081.

[28] Z. Zhao, A. El-Naggar, J. Kau, C. Olson, D. Tomlinson, S.X. Chang, Biochar affects compressive strength of Portland cement composites: a meta-analysis, Biochar 6 (2024) 21. https://doi.org/10.1007/s42773-024-00309-2.

[29] P. Zhao, H. Qie, X. Cui, W. Zhang, T. Pu, W. Bao, X. Li, A. Lin, M. Ren, The effect of interfering ions on the degradation of organic pollutants by two types of activated persulfates over Fe-based catalysts in water: A meta-analysis, Chemical Engineering Journal 509 (2025) 161123. https://doi.org/10.1016/j.cej.2025.161123.

[30] N. Nitta, F. Wu, J.T. Lee, G. Yushin, Li-ion battery materials: present and future, Materials Today 18 (2015) 252–264. https://doi.org/10.1016/j.mattod.2014.10.040.

[31] J. Guo, P. Li, F. Piccolo, Y. Jie, H. Jia, R. Cao, S. Jiao, P. Adelhelm, Y. Xu, Degradation and Failure Mechanisms of Lithium/LiNi x Co y Mn 1– x – y O 2 Batteries, ACS Energy Letters 10 (2025) 2318–2340. https://doi.org/10.1021/acsenergylett.4c03578.

[32] H. Du, Y. Wang, Y. Kang, Y. Zhao, Y. Tian, X. Wang, Y. Tan, Z. Liang, J. Wozny, T. Li, D. Ren, L. Wang, X. He, P. Xiao, E. Mao, N. Tavajohi, F. Kang, B. Li, Side Reactions/Changes in Lithium-Ion Batteries: Mechanisms and Strategies for Creating Safer and Better Batteries, Advanced materials 36 (2024) e2401482. https://doi.org/10.1002/adma.202401482.

[33] T. Havránek, T.D. Stanley, H. Doucouliagos, P. Bom, J. Geyer‐Klingeberg, I. Iwasaki, W.R. Reed, K. Rost, R.C.M. van Aert, Reporting guidelines for meta-analysis in economics, Journal of Economic Surveys 34 (2020) 469–475. https://doi.org/10.1111/joes.12363.

[34] W.S. Richardson, C.M. Wilson, J. Nishikawa, S.R. Hayward, The well-built clinical question: a key to evidence-based decisions, ACP Journal Club 123 (1995) A12-A13. https://doi.org/10.7326/ACPJC-1995-123-3-A12.

[35] The Campbell Collaboration, Campbell Collaboration Systematic Reviews: Policies and Guidelines, 2021.

[36] V. Sulzer, P. Mohtat, A. Aitio, S. Lee, Y.T. Yeh, F. Steinbacher, M.U. Khan, J.W. Lee, J.B. Siegel, A.G. Stefanopoulou, D.A. Howey, The challenge and opportunity of battery lifetime prediction from field data, Joule 5 (2021) 1934–1955. https://doi.org/10.1016/j.joule.2021.06.005.

[37] H. Rauf, M. Khalid, N. Arshad, Machine learning in state of health and remaining useful life estimation: Theoretical and technological development in battery degradation modelling, Renewable and Sustainable Energy Reviews 156 (2022) 111903. https://doi.org/10.1016/j.rser.2021.111903.

[38] C.R. Birkl, M.R. Roberts, E. McTurk, P.G. Bruce, D.A. Howey, Degradation diagnostics for lithium ion cells, Journal of Power Sources 341 (2017) 373–386. https://doi.org/10.1016/j.jpowsour.2016.12.011.

[39] P.M. Attia, A. Bills, F. Brosa Planella, P. Dechent, G. dos Reis, M. Dubarry, P. Gasper, R. Gilchrist, S. Greenbank, D. Howey, O. Liu, E. Khoo, Y. Preger, A. Soni, S. Sripad, A.G. Stefanopoulou, V. Sulzer, Review—"Knees" in Lithium-Ion Battery Aging Trajectories, Journal of The Electrochemical Society 169 (2022) 60517. https://doi.org/10.1149/1945-7111/ac6d13.

[40] T.A. Craney, J.G. Surles, Model-Dependent Variance Inflation Factor Cutoff Values, Quality Engineering 14 (2002) 391–403. https://doi.org/10.1081/QEN-120001878.

[41] T. Havranek, Z. Irsova, Estimating vertical spillovers from FDI: Why results vary and what the true effect is, Journal of International Economics 85 (2011) 234–244. https://doi.org/10.1016/j.jinteco.2011.07.004.

[42] M.B. Nuijten, M.A.L.M. van Assen, H.E.M. Augusteijn, E.A.V. Crompvoets, J.M. Wicherts, Effect Sizes, Power, and Biases in Intelligence Research: A Meta-Meta-Analysis, J. Intell. 8 (2020). https://doi.org/10.3390/jintelligence8040036.

[43] J.C. Clements, J. Sundin, T.D. Clark, F. Jutfelt, Meta-analysis reveals an extreme "decline effect" in the impacts of ocean acidification on fish behavior, PLoS Biol. 20 (2022) e3001511. https://doi.org/10.1371/journal.pbio.3001511.

[44] J. Xie, K. Gong, Y. Cheng, Q. Ke, The correlation between paper length and citations: a meta-analysis, Scientometrics 118 (2019) 763–786. https://doi.org/10.1007/s11192-019-03015-0.

[45] T.D. Stanley, S.B. Jarrell, Meta-Regression Analysis: A Quantitative Method of Literature Surveys, Journal of Economic Surveys 3 (1989) 161–170. https://doi.org/10.1111/j.1467-6419.1989.tb00064.x.

[46] Z. Irsova, H. Doucouliagos, T. Havranek, T.D. Stanley, Meta-analysis of social science research: A practitioner's guide, Journal of Economic Surveys 38 (2024) 1547–1566. https://doi.org/10.1111/joes.12595.

[47] J.A. Hoeting, D. Madigan, A.E. Raftery, C.T. Volinsky, Bayesian model averaging: a tutorial (with comments by M. Clyde, David Draper and E. I. George, and a rejoinder by the authors, Statistical Science 14 (1999) 382–401. https://doi.org/10.1214/ss/1009212519.

[48] N. Döbbeling-Hildebrandt, K. Miersch, T.M. Khanna, M. Bachelet, S.B. Bruns, M. Callaghan, O. Edenhofer, C. Flachsland, P.M. Forster, M. Kalkuhl, N. Koch, W.F. Lamb, N. Ohlendorf, J.C. Steckel, J.C. Minx, Systematic review and meta-analysis of ex-post evaluations on the effectiveness of carbon pricing, Nat. Commun. 15 (2024) 4147. https://doi.org/10.1038/s41467-024-48512-w.

[49] K. Kroupova, T. Havranek, Z. Irsova, Student Employment and Education: A Meta-Analysis, Economics of Education Review 100 (2024) 102539. https://doi.org/10.1016/j.econedurev.2024.102539.

[50] M. Schütt, Wind Turbines and Property Values: A Meta-Regression Analysis, Environmental and Resource Economics 87 (2024) 1–43. https://doi.org/10.1007/s10640-023-00809-y.

[51] Z. Sun, D. Zhu, Investigating environmental regulation effects on technological innovation: A meta-regression analysis, Energy & Environment 34 (2023) 463–492. https://doi.org/10.1177/0958305X211069654.

[52] M. Hinne, Q.F. Gronau, D. van den Bergh, E.-J. Wagenmakers, A Conceptual Introduction to Bayesian Model Averaging, Advances in Methods and Practices in Psychological Science 3 (2020) 200–215. https://doi.org/10.1177/2515245919898657.

[53] E.I. George, Dilution priors: Compensating for model space redundancy, in: J.O. Berger, T.T. Cai, I.M. Johnstone (Eds.), Borrowing Strength: Theory Powering Applications – A Festschrift for Lawrence D. Brown, Institute of Mathematical Statistics, Beachwood, Ohio, USA, 2010, pp. 158–165.

[54] R.E. Kass, L. Wasserman, A Reference Bayesian Test for Nested Hypotheses and its Relationship to the Schwarz Criterion, Journal of the American Statistical Association 90 (1995) 928. https://doi.org/10.2307/2291327.

[55] J.-L.J. Geyer-Klingeberg, Meta-Analysis in Finance: Applications and Advances. Dissertation Thesis, Augsburg, 2022.

[56] L. Tan, L. Zhang, Q. Sun, M. Shen, Q. Qu, H. Zheng, Capacity loss induced by lithium deposition at graphite anode for LiFePO4/graphite cell cycling at different temperatures, Electrochimica Acta 111 (2013) 802–808. https://doi.org/10.1016/j.electacta.2013.08.074.

[57] W. Black, S. Azam, H. MacLennan, M. Metzger, J.R. Dahn, Understanding Capacity Loss in LFP/Graphite Pouch Cells at High Temperatures through Modelling, Journal of The Electrochemical Society 172 (2025) 90503. https://doi.org/10.1149/1945-7111/adf5ed.

[58] S. Azam, W. Black, H. MacLennan, A. Eldesoky, J.R. Dahn, Additive Screening of LFP/graphite Pouch Cells for High Temperature Cycling at 70 °C, Journal of The Electrochemical Society 172 (2025) 20536. https://doi.org/10.1149/1945-7111/adb64d.

[59] I. Buchmann, BU-205: Types of Lithium-ion, 2010. https://batteryuniversity.com/article/bu-205-types-of-lithium-ion (accessed 2 September 2025).

[60] Z.-W. Gao, T. Lan, H. Yin, Y. Liu, Development and Commercial Application of Lithium-Ion Batteries in Electric Vehicles: A Review, Processes 13 (2025) 756. https://doi.org/10.3390/pr13030756.

[61] T. Abe, SECONDARY BATTERIES – LITHIUM RECHARGEABLE SYSTEMS – LITHIUM-ION | Negative Electrodes: Carbon, in: J. Garche (Ed.), Encyclopedia of electrochemical power sources, Elsevier Academic Press, Amsterdam, Heidelberg, 2009, pp. 192–197.

[62] J. Yao, G.X. Wang, J. Ahn, H.K. Liu, S.X. Dou, Electrochemical studies of graphitized mesocarbon microbeads as an anode in lithium-ion cells, Journal of Power Sources 114 (2003) 292–297. https://doi.org/10.1016/S0378-7753(02)00585-2.

[63] A. Kampker, H.H. Heimes, Elektromobilität, Springer Berlin Heidelberg, Berlin, Heidelberg, 2024.

[64] X.H. Liu, L. Zhong, S. Huang, S.X. Mao, T. Zhu, J.Y. Huang, Size-dependent fracture of silicon nanoparticles during lithiation, ACS Nano 6 (2012) 1522–1531. https://doi.org/10.1021/nn204476h.

[65] H. Zhang, Y. Yang, H. Xu, L. Wang, X. Lu, X. He, 2022. Li 4 Ti 5 O 12 spinel anode: Fundamentals and advances in rechargeable batteries. InfoMat 4, e12228. https://doi.org/10.1002/inf2.12228.

[66] L. Lu, X. Han, J. Li, J. Hua, M. Ouyang, A review on the key issues for lithium-ion battery management in electric vehicles, Journal of Power Sources 226 (2013) 272–288. https://doi.org/10.1016/j.jpowsour.2012.10.060.

[67] S. Baazouzi, N. Feistel, J. Wanner, I. Landwehr, A. Fill, K.P. Birke, Design, Properties, and Manufacturing of Cylindrical Li-Ion Battery Cells—A Generic Overview, Batteries 9 (2023) 309. https://doi.org/10.3390/batteries9060309.

[68] S. Link, C. Neef, T. Wicke, Trends in Automotive Battery Cell Design: A Statistical Analysis of Empirical Data, Batteries 9 (2023) 261. https://doi.org/10.3390/batteries9050261.

[69] H. Löbberding, S. Wessel, C. Offermanns, M. Kehrer, J. Rother, H. Heimes, A. Kampker, From Cell to Battery System in BEVs: Analysis of System Packing Efficiency and Cell Types, WEVJ 11 (2020) 77. https://doi.org/10.3390/wevj11040077.

[70] N. Saber, C.P. Richter, R. Unnthorsson, Review of Thermal Management Techniques for Prismatic Li-Ion Batteries, Energies 18 (2025) 492. https://doi.org/10.3390/en18030492.

[71] S. Link, C. Neef, T. Wicke, T. Hettesheimer, M. Diehl, O. Krätzig, F. Degen, F. Klein, P. Fanz, M. Burgard, R. Kleinert, Development perspectives for lithium-ion battery cell formats, Fraunhofer-Gesellschaft, 2021.

[72] M.W. Marzook, J. Eaton, M.A. Samieian, Y. Patel, G. Offer, M. Marinescu, The effect of test conditions on the relative performance of cylindrical lithium-ion cells, Journal of Energy Storage 105 (2025) 114485. https://doi.org/10.1016/j.est.2024.114485.

[73] R.-G. Scurtu, A. Innocenti, V. Scheck, M. Maunz, T. Waldmann, M. Hölzle, A. Hoffmann, P. Axmann, M. Wohlfahrt-Mehrens, From small batteries to big claims, Nat. Nanotechnol. 20 (2025) 970–976. https://doi.org/10.1038/s41565-025-01906-3.

[74] F. Dai, M. Cai, Best practices in lithium battery cell preparation and evaluation, Communications Materials 3 (2022). https://doi.org/10.1038/s43246-022-00286-8.

[75] K. Chen, J. Luo, Y. Huang, Impact of low temperature exposure on lithium-ion batteries: A multi-scale study of performance degradation, predictive signals and underlying mechanisms, Chemical Engineering Journal 503 (2025) 158260. https://doi.org/10.1016/j.cej.2024.158260.

[76] M.-T.F. Rodrigues, G. Babu, H. Gullapalli, K. Kalaga, F.N. Sayed, K. Kato, J. Joyner, P.M. Ajayan, A materials perspective on Li-ion batteries at extreme temperatures, Nature Energy 2 (2017). https://doi.org/10.1038/nenergy.2017.108.

[77] A. Belgibayeva, A. Rakhmetova, M. Rakhatkyzy, M. Kairova, I. Mukushev, N. Issatayev, G. Kalimuldina, A. Nurpeissova, Y.-K. Sun, Z. Bakenov, Lithium-ion batteries for low-temperature applications: Limiting factors and solutions, Journal of Power Sources 557 (2023) 232550. https://doi.org/10.1016/j.jpowsour.2022.232550.

[78] S. Zhang, K. Xu, T.R. Jow, A new approach toward improved low temperature performance of Li-ion battery, Electrochemistry Communications 4 (2002) 928–932. https://doi.org/10.1016/S1388-2481(02)00490-3.

[79] Z. Gao, H. Xie, X. Yang, W. Niu, S. Li, S. Chen, The Dilemma of C-Rate and Cycle Life for Lithium-Ion Batteries under Low Temperature Fast Charging, Batteries 8 (2022) 234. https://doi.org/10.3390/batteries8110234.

[80] J. Vetter, P. Novák, M.R. Wagner, C. Veit, K.-C. Möller, J.O. Besenhard, M. Winter, M. Wohlfahrt-Mehrens, C. Vogler, A. Hammouche, Ageing mechanisms in lithium-ion batteries, Journal of Power Sources 147 (2005) 269–281. https://doi.org/10.1016/j.jpowsour.2005.01.006.

[81] F. Leng, C.M. Tan, M. Pecht, Effect of Temperature on the Aging rate of Li Ion Battery Operating above Room Temperature, Sci. Rep. 5 (2015) 12967. https://doi.org/10.1038/srep12967.

[82] D. Ren, X. Feng, L. Lu, X. He, M. Ouyang, Overcharge behaviors and failure mechanism of lithium-ion batteries under different test conditions, Applied Energy 250 (2019) 323–332. https://doi.org/10.1016/j.apenergy.2019.05.015.

[83] H. He, Y. Liu, Q. Liu, Z. Li, F. Xu, C. Dun, Y. Ren, M. Wang, J. Xie, Failure Investigation of LiFePO 4 Cells in Over-Discharge Conditions, Journal of The Electrochemical Society 160 (2013) A793-A804. https://doi.org/10.1149/2.039306jes.

[84] L. Zhang, Y. Ma, X. Cheng, C. Du, T. Guan, Y. Cui, S. Sun, P. Zuo, Y. Gao, G. Yin, Capacity fading mechanism during long-term cycling of over-discharged LiCoO2/mesocarbon microbeads battery, Journal of Power Sources 293 (2015) 1006–1015. https://doi.org/10.1016/j.jpowsour.2015.06.040.

[85] D. Ouyang, J. Weng, M. Chen, J. Wang, Impacts of Current Rates on the Degradation Behaviors of Lithium-Ion Batteries under Over-Discharge Conditions, Journal of The Electrochemical Society 166 (2019) A3432-A3440. https://doi.org/10.1149/2.1131914jes.

[86] Y. Gao, J. Jiang, C. Zhang, W. Zhang, Z. Ma, Y. Jiang, Lithium-ion battery aging mechanisms and life model under different charging stresses, Journal of Power Sources 356 (2017) 103–114. https://doi.org/10.1016/j.jpowsour.2017.04.084.

[87] D. Ouyang, J. Weng, M. Chen, J. Wang, Impact of high-temperature environment on the optimal cycle rate of lithium-ion battery, Journal of Energy Storage 28 (2020) 101242. https://doi.org/10.1016/j.est.2020.101242.

[88] G. Kucinskis, M. Bozorgchenani, M. Feinauer, M. Kasper, M. Wohlfahrt-Mehrens, T. Waldmann, Arrhenius plots for Li-ion battery ageing as a function of temperature, C-rate, and ageing state – An experimental study, Journal of Power Sources 549 (2022) 232129. https://doi.org/10.1016/j.jpowsour.2022.232129.

[89] S. Hong, Citizen Participation in Budgeting: A Trade-Off between Knowledge and Inclusiveness?, Public Administration Review 75 (2015) 572–582. https://doi.org/10.1111/puar.12377.

[90] C. Candolo, A.C. Davison, C.G.B. Demétrio, A note on model uncertainty in linear regression, Journal of the Royal Statistical Society: Series D (The Statistician) 52 (2003) 165–177. https://doi.org/10.1111/1467-9884.00349.

[91] W. Li, B. Song, A. Manthiram, High-voltage positive electrode materials for lithium-ion batteries, Chem. Soc. Rev. 46 (2017) 3006–3059. https://doi.org/10.1039/C6CS00875E.

[92] K. Guo, S. Qi, H. Wang, J. Huang, M. Wu, Y. Yang, X. Li, Y. Ren, J. Ma, High-Voltage Electrolyte Chemistry for Lithium Batteries, Small Sci. 2 (2022) 2100107. https://doi.org/10.1002/smsc.202100107.

[93] F. Wang, S. Tang, X. Han, Y. Wu, L. Lu, C. Yu, X. Sun, M. Ouyang, Flexible upper cut-off voltage regulation for life extension of lithium-ion batteries, Energy 318 (2025) 134776. https://doi.org/10.1016/j.energy.2025.134776.

[94] C.B. Begg, J.A. Berlin, Publication Bias: A Problem in Interpreting Medical Data, Journal of the Royal Statistical Society. Series A (Statistics in Society) 151 (1988) 419. https://doi.org/10.2307/2982993.

[95] T.D. Stanley, S.B. Jarrell, Meta-Regression Analysis: A Quantitative Method of Literature Surveys, Journal of Economic Surveys 19 (2005) 299–308. https://doi.org/10.1111/j.0950-0804.2005.00249.x.

[96] M. Egger, G. Davey Smith, M. Schneider, C. Minder, Bias in meta-analysis detected by a simple, graphical test, British Medical Journal 315 (1997) 629–634. https://doi.org/10.1136/bmj.315.7109.629.

[97] A. Franco, N. Malhotra, G. Simonovits, Social science. Publication bias in the social sciences: unlocking the file drawer, Science 345 (2014) 1502–1505. https://doi.org/10.1126/science.1255484.

[98] J.P.A. Ioannidis, Why most published research findings are false, PLoS Med. 2 (2005) e124. https://doi.org/10.1371/journal.pmed.0020124.

[99] R. Huang, G. Wei, X. Wang, B. Jiang, J. Zhu, J. Chen, X. Wei, H. Dai, Revealing the low-temperature aging mechanisms of the whole life cycle for lithium-ion batteries (nickel-cobalt-aluminum vs. graphite), Journal of Energy Chemistry 106 (2025) 31–43. https://doi.org/10.1016/j.jechem.2025.02.043.

[100] S.-J. Kwon, S.-E. Lee, J.-H. Lim, J. Choi, J. Kim, Performance and Life Degradation Characteristics Analysis of NCM LIB for BESS, Electronics 7 (2018) 406. https://doi.org/10.3390/electronics7120406.

[101] Y. Li, K. Qian, Y.-B. He, Y.V. Kaneti, D. Liu, D. Luo, H. Li, B. Li, F. Kang, Study on the reversible capacity loss of layered oxide cathode during low-temperature operation, Journal of Power Sources 342 (2017) 24–30. https://doi.org/10.1016/j.jpowsour.2016.12.033.

[102] R. Wittman, M. Dubarry, S. Ivanov, B.W. Juba, J. Romàn-Kustas, A. Fresquez, J. Langendorf, R. Grant, G. Taggart, B. Chalamala, Y. Preger, Characterization of Cycle-Aged Commercial NMC and NCA Lithium-ion Cells: I. Temperature-Dependent Degradation, Journal of The Electrochemical Society 170 (2023) 120538. https://doi.org/10.1149/1945-7111/ad1450.

[103] C.P. Aiken, E.R. Logan, A. Eldesoky, H. Hebecker, J.M. Oxner, J.E. Harlow, M. Metzger, J.R. Dahn, Li[Ni 0.5 Mn 0.3 Co 0.2]O 2 as a Superior Alternative to LiFePO 4 for Long-Lived Low Voltage Li-Ion Cells, Journal of The Electrochemical Society 169 (2022) 50512. https://doi.org/10.1149/1945-7111/ac67b5.

[104] S. Evro, A. Ajumobi, D. Mayon, O.S. Tomomewo, Navigating battery choices: A comparative study of lithium iron phosphate and nickel manganese cobalt battery technologies, Future Batteries 4 (2024) 100007. https://doi.org/10.1016/j.fub.2024.100007.

[105] M.R. Palacín, A. de Guibert, Why do batteries fail?, Science 351 (2016) 1253292. https://doi.org/10.1126/science.1253292.

[106] B. Li, J. Xiao, X. Zhu, Z. Wu, X. Zhang, Y. Han, J. Niu, F. Wang, Enabling high-performance lithium iron phosphate cathodes through an interconnected carbon network for practical and high-energy lithium-ion batteries, J. Colloid Interface Sci. 653 (2024) 942–948. https://doi.org/10.1016/j.jcis.2023.09.133.

[107] H. Shobukawa, J. Alvarado, Y. Yang, Y.S. Meng, Electrochemical performance and interfacial investigation on Si composite anode for lithium ion batteries in full cell, Journal of Power Sources 359 (2017) 173–181. https://doi.org/10.1016/j.jpowsour.2017.05.044.

[108] Y. Guo, M. Miao, Y.-X. Wang, C. Yan, J. Liu, Y. Cao, H. Yang, X. Ai, F.-S. Ke, A high-voltage and low-solvating electrolyte towards promising micro-Si/Ni-rich NMC full cells, Energy Storage Materials 67 (2024) 103258. https://doi.org/10.1016/j.ensm.2024.103258.

[109] S. Hasselwander, M. Meyer, I. Österle, Techno-Economic Analysis of Different Battery Cell Chemistries for the Passenger Vehicle Market, Batteries 9 (2023) 379. https://doi.org/10.3390/batteries9070379.

[110] Y. Ding, Z.P. Cano, A. Yu, J. Lu, Z. Chen, Automotive Li-Ion Batteries: Current Status and Future Perspectives, Electrochemical Energy Reviews 2 (2019) 1–28. https://doi.org/10.1007/s41918-018-0022-z.

[111] I.T. Adebanjo, J. Eko, A.G. Agbeyegbe, S.F. Yuk, S.V. Cowart, E.A. Nagelli, F.J. Burpo, J.L. Allen, D.T. Tran, N. Bhattarai, K. Shah, J.-Y. Hwang, H.H. Sun, A comprehensive review of lithium-ion battery components degradation and operational considerations: a safety perspective, Energy Advances 4 (2025) 820–877. https://doi.org/10.1039/D5YA00065C.

Graphical Abstract

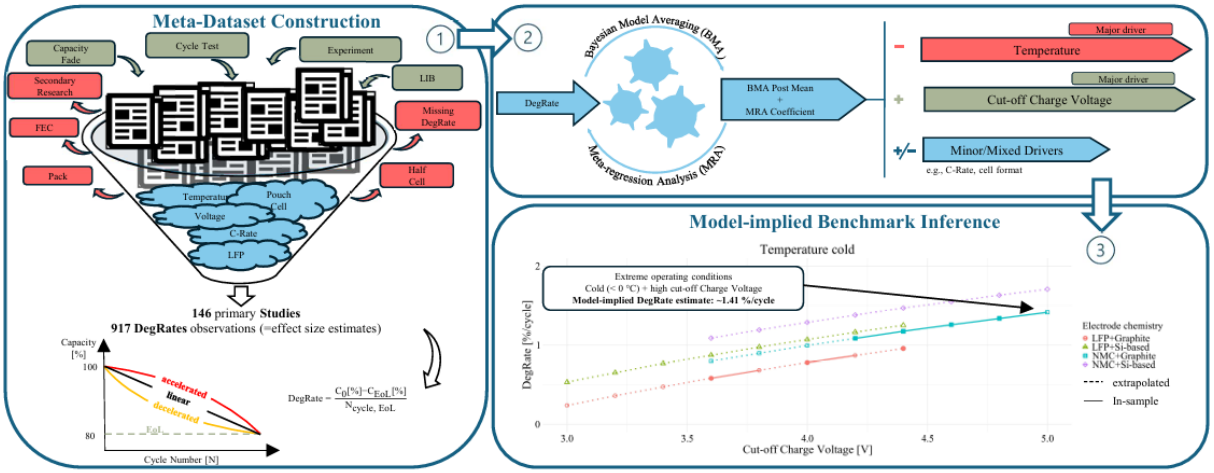

Statements

Declaration of competing interest

The authors declare that they have no known competing financial interests or personal relationships that could have appeared to influence the work reported in this paper.

Data availability

The data for this paper is uploaded as supplementary material to this submission.

Funding sources

This research did not receive any specific grant from funding agencies in the public, commercial, or not-for-profit sectors.

Declaration of generative AI and AI-assisted technologies in the writing process

During the preparation of this work the authors used ChatGPT in order to improve the readability and language of the manuscript. After using this tool/service, the authors reviewed and edited the content as needed and take full responsibility for the content of the published article.

Acknowledgements

The authors would like to thank the participants of the MAERNET 2024, ICSET 2025, EUPVSEC 2025 and the seminar participants at the University of Augsburg, for their valuable discussion and comments.

CRediT authorship contribution statement

Matteo Ligorati: Conceptualization, Data curation, Investigation, Methodology, Formal analysis, Software, Validation, Visualization, Writing – original draft, Writing – review & editing. **Jerome Geyer-Klingeberg**: Conceptualization, Methodology, Formal analysis, Software, Supervision, Writing – original draft, Writing – review & editing. **Timon E. Günther:** Conceptualization, Investigation, Visualization, Writing – original draft **Andreas W. Rathgeber**: Conceptualization, Formal analysis, Supervision, Writing – review & editing.

Highlights of

Degradation of lithium-ion batteries: a meta-analysis

Matteo Ligorati[a], Jerome Geyer-Klingeberg[a], Timon E. Günther[b], and Andreas W. Rathgeber[a]

[a] Professorship for Applied Data Analysis, Institute of Materials Resource Management, University of Augsburg, Am Technologiezentrum 8, 86159 Augsburg, Germany

[b] Department of Resource and Chemical Engineering, Institute of Materials Resource Management, University of Augsburg, Am Technologiezentrum 8, 86159 Augsburg, Germany

˜Corresponding author: matteo.ligorati@uni-a.de (M. Ligorati), Tel.: +49 821 598 – 69205

Highlights

- Analysis of 146 lithium-ion battery cycle studies between 2006 and 2024.
- Median and mean capacity degradation rates of 0.04 %/cycle and 0.23 %/cycle.
- Key drivers: test conditions, defects, degradation curve, manufacturer origin.
- Quantitative benchmark for degradation under untested operating conditions.
- Extreme test conditions: 0.68–1.41 %/cycle fading in graphite-based cells.